shRNA expression vector and anti-SOD1 shRNA transgenic mice as reported previously [11,12]. In brief, we inserted anti-SOD1 shRNA driven by human U6 promoter into pUC19 (Takara). The shRNA expression vector was introduced into the 129/Sv embryonic stem (ES) cells (Chemicon) by electroporation. The ES cell clones in which SOD1 protein levels were effectively suppressed were introduced into C57BL/6 blastocysts (CLEA) by microinjection. We obtained F1 transgenic mice by crossing the chimeric male mice with wild-type C57BL/6 female mice.

2.2. Histological study

To analyze hepatic lipid accumulation, liver samples from 8-month-old shRNA transgenic male mice and wild-type littermates were sectioned (4 μm) and fixed in 4% paraformaldehyde/phosphate-buffered saline (PBS) for 5 min, and then stained with filtrated Sudan III (Muto pure chemicals) at 37 °C for 30 min. Counterstaining of nuclei was performed with Mayer hematoxylin solution (Muto pure chemicals) for 3 min.

2.3. Western blot analysis

Western blot analysis was performed as reported previously [11]. Mice were killed under anesthesia with pentobarbital sodium, and perfused with cold PBS. Tissues were homogenized in the cold buffer containing 0.1% sodium dodecyl sulfate (SDS), 1% sodium deoxycholate, 1% Triton X-100, 1 mM phenylmethylsulfonyl fluoride and protease inhibitor cocktail (Sigma). Equal amounts of protein from each sample were loaded in the assays. The separated proteins were detected by specific primary antibodies; rabbit anti-SOD1 antibody (1:5000, StressGen Biotechnologies), mouse anti-β-tubulin antibody (1:1000, BD Biosciences), mouse anti-Actin antibody (1:1000, Santa Cruz Biotechnology), mouse anti-Ago2 antibody (1:500, Abcam), or rabbit anti-N-ras antibody (1:500, Santa Cruz Biotechnology).

2.4. Northern blot analysis

Northern blot analysis was performed as reported previously [11]. Ten micrograms of total RNA from each sample were loaded in the assays. The DNA probes which were used to detect RNAs were as follows; complementary DNA (cDNA) (bases 15–495) for mouse SOD1; cDNA (bases 300–614) for mouse glyceraldehyde-3-phosphate dehydrogenase (GAPDH); 5′-GGTGGAAATGAAGAAA-GTAC-3′ for anti-SOD1 siRNA guide strand; 5′-ACTATACAACCTAC-TACCTCA-3′ for mouse let-7a; 5′-GGCATTCACCGCGTGCCTTA-3′ for mouse miR-124a; 5′-AAATATGGAACGCTTCACGA-3′ for mouse U6 small nuclear RNA (snRNA).

2.5. Quantitative reverse transcription polymerase chain reaction (RT-PCR)

After treating with TURBO DNA-free (Ambion) to remove residual genomic DNA, 1 μg of total RNA from each sample was reversely transcribed to cDNA using SuperScript III Reverse Transcriptase (Invitrogen). The cDNA was used for quantitative PCR with TaqMan system using the ABI Prism 7700 Sequence Detection System (Applied Biosystems) according to the manufacturer's protocol. The primers and probe used to quantify mouse SOD1 were 5′-GGTGCAGGGAACCATCCA-3′ for forward primer, 5′-CCCATGCTGGCCTTCAGT-3′ for reverse primer, and 5′-AGGCA-AGCGGTGAACCAGTTGTGTTG-3′ for probe. The primer and probe sets of mouse GAPDH, N-ras and N-myc were purchased from Applied Biosystems. GAPDH was used to normalize the quantitative RT-PCR values.

2.6. Laser microdissection and RNA extraction from motor neurons and non-neuronal cells

Collection of motor neurons and non-neuronal cells was performed as reported previously [13]. Spinal cords of the transgenic mice or wild-type littermates were removed and embedded in Tissue-Tek O.C.T. Compound (Sakura Finetek). Seven micrometer thick sections were mounted on a MembraneSlide (Leica) and stained with HistoGene staining solution (Arcturus). Approximate one thousand motor neurons and neighboring non-neuronal cells were dissected from the ventral horn of the lumbar spinal cord for each mouse using an AS LMD system (Leica). Total RNA was extracted using RNeasy Micro Kit (Qiagen) according to the manufacturer's protocol.

2.7. Subcellular fractionation

Subcellular fractionation was performed as described previously [14]. The cerebrum or liver was gently homogenized in cold buffer (0.22 M D-mannitol, 0.07 M sucrose, at 1 mg tissue/10 μl buffer) with a glass-Teflon homogenizer (30 up-and-down strokes), and centrifuged at 600×g for 10 min. The pellets were suspended with 2.2 M sucrose and centrifuged at 40000×g for 1 h. The resulting pellets were used as nuclear fraction. The supernatants generated by the first centrifugation were used as cytoplasmic fraction. Total RNA was extracted using ISOGEN (Nippon Gene) for nuclear fraction and ISOGEN-LS (Nippon Gene) for cytoplasmic fraction, respectively.

2.8. Statistical analysis

Student's *t*-test was used to evaluate difference among tissues or difference between transgenic mice and wild-type littermates. Significance was set at $P < 0.05$. To compare the expression level on Western blot or Northern blot analysis, we used NIH ImageJ to quantify the band intensity.

3. Results

3.1. Anti-SOD1 shRNA transgenic mice recapitulate SOD1-null mice

As reported previously, we obtained anti-SOD1 shRNA transgenic mice (Fig. 1A) [11]. The silencing effect of the target gene was significant on both RNA and protein levels, and was stable with age and through to the F3 generation [11]. In contrast, there was no change in the expression levels of unrelated genes including GAPDH and β-actin ($P = 0.75$ and 0.27, respectively, data not shown). The transgenic mice showed no remarkable phenotype during development. The adult mice exhibited mild fatty liver (Fig. 1B and C) and female infertility (data not shown), which were also observed in SOD1-null mice [15,16]. These findings indicate that the phenotype of the anti-SOD1 shRNA transgenic mice is similar to that of SOD1-null mice.

3.2. The siRNA-silencing efficiency differs among the tissues of the shRNA transgenic mice

We analyzed the siRNA-silencing efficiency in the various tissues of the shRNA transgenic mice. On Western blot analysis, we observed marked suppression of SOD1 protein in all the tissues examined (Fig. 2A). However, the siRNA-silencing efficiency was clearly different among the tissues; it was extremely high in the liver and skeletal muscle (>95%) and, in contrast, was relatively low in the central nervous system and lung (~80%) (Fig. 2A and B). The

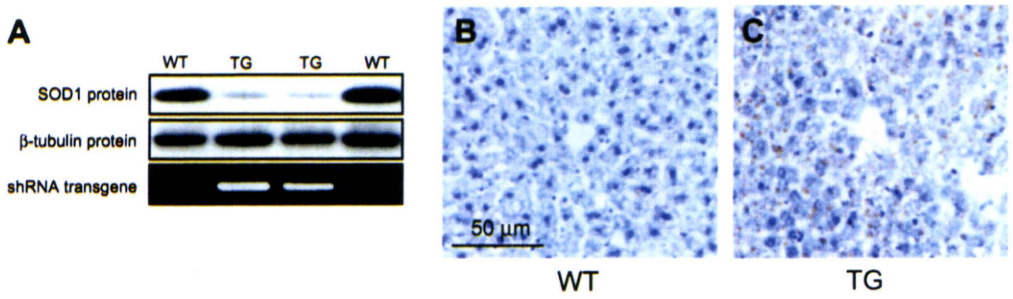

Fig. 1. Generation of anti-SOD1 shRNA transgenic mice. (A) Western blot analysis of SOD1 (upper) and β-tubulin (middle), and genomic PCR of transgene (lower) in the tails. Histological analysis in the liver of the wild-type littermates (B) and shRNA transgenic mice (C). The sections were stained with Sudan III. WT, age-matched wild-type littermates; TG, transgenic mice.

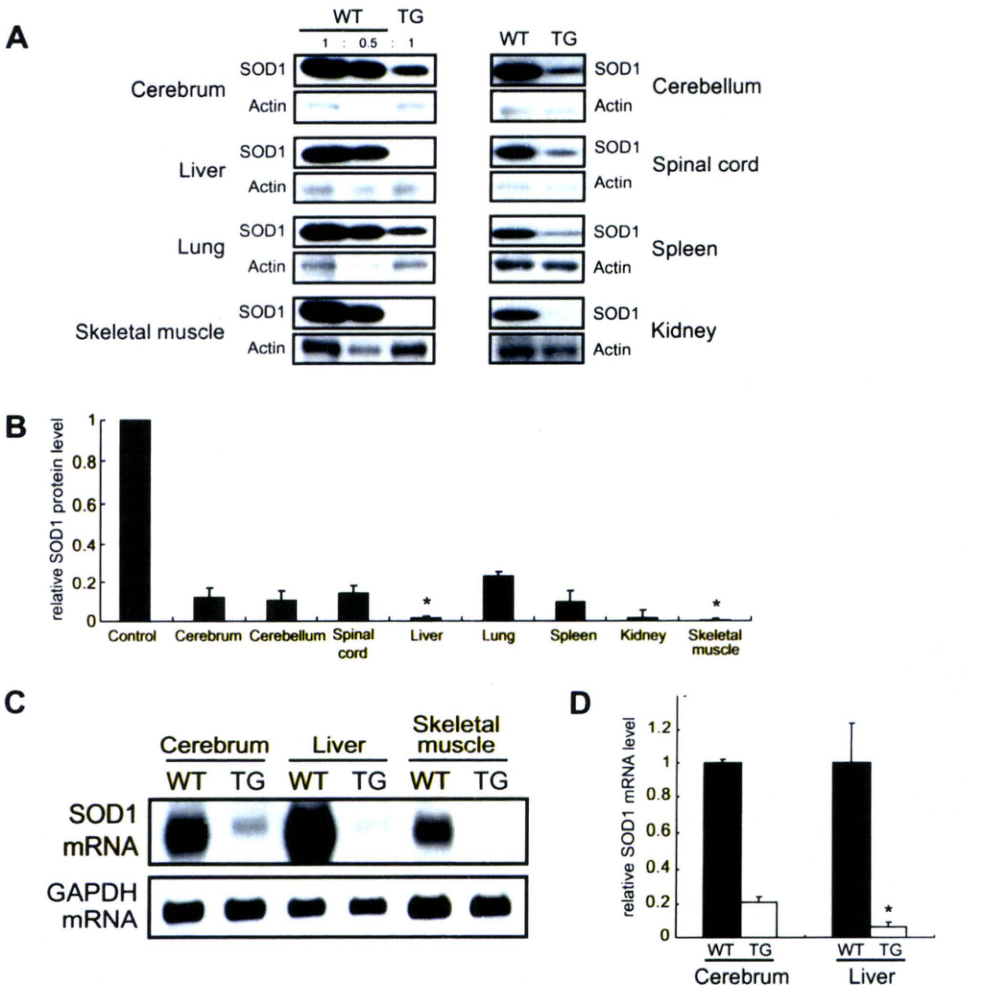

Fig. 2. Silencing efficiency in the various tissues of the shRNA transgenic mice. (A) SOD1 protein levels on Western blot analysis in the tissues of the transgenic mice. A half amounts of the wild-type samples are loaded in the middle lanes of left panel to show that the signals are not saturated. (B) Quantification of their band intensities. Values are the ratio to those of age-matched wild-type littermates (mean and S.D., $n = 3$, $^{*}P < 0.05$; significance compared to cerebrum). (C) SOD1 mRNA of the cerebrum, liver and skeletal muscle on Northern blot analysis. (D) Quantitative RT-PCR of SOD1 mRNA in the cerebrum and liver. Values are the ratio to age-matched wild-type littermates (mean and S.D., $n = 3$, $^{*}P < 0.05$; significance compared to cerebrum).

difference was also confirmed on RNA level by Northern blot analysis (Fig. 2C) and quantitative RT-PCR (Fig. 2D).

3.3. The siRNA-silencing efficiency in neuronal cells is relatively lower than those in hepatocytes and muscle fibers

Because central nervous system is composed of heterogenous cell populations, we sought to evaluate the siRNA-silencing efficiency in neuronal and non-neuronal cells using laser microdissection method. The motor neurons and non-neuronal cells were isolated from the ventral horn of the lumbar spinal cords in the shRNA transgenic mice or wild-type littermates (Fig. 3A–D), and SOD1 mRNA levels were quantified by quantitative RT-PCR. The silencing efficiency in the motor neurons was approximately 80% which was similar to the non-neuronal cells (Fig. 3E) and the whole spinal cord tissue (Fig. 2B), and was less than those in the liver and

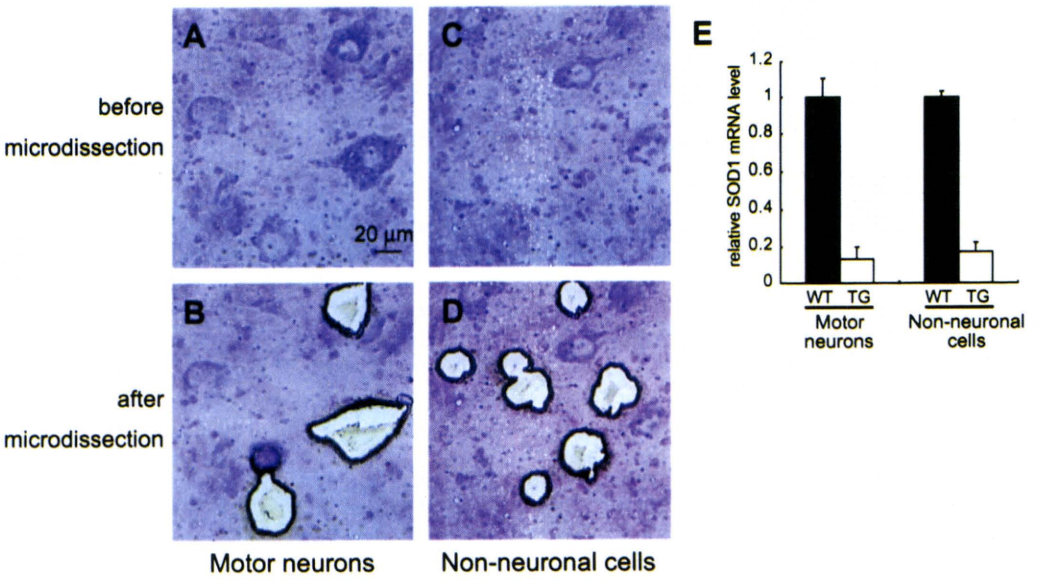

Fig. 3. Silencing efficiency in the neuronal and non-neuronal cells of the shRNA transgenic mice. (A–D) Microdissection of motor neurons and non-neuronal cells in the ventral horn of the lumbar spinal cord of the transgenic mice and age-matched wild-type littermates. Motor neurons (A and B) and non-neuronal cells (C and D) were dissected by laser microbeam. (E) Quantification of SOD1 mRNA in the motor neurons and non-neuronal cells by quantitative RT-PCR (mean and S.D., $n = 3$).

skeletal muscle (Fig. 2B). Since liver and skeletal muscle are mostly composed of hepatocytes and muscle fibers, respectively, these results indicate that the siRNA-silencing efficiency is different among cell populations in the shRNA transgenic mice.

3.4. The mechanism of tissue difference in siRNA-silencing efficiency

In order to study the mechanism of this tissue difference in siRNA-silencing efficiency, we first analyzed the expression levels of shRNA and siRNA with the probe to the guide strand of siRNA, and compared them to the expression level of the target mRNA in each tissue. The 54 mer shRNA was not detected in any tissue (data not shown), indicating that processing of shRNA by Dicer is excellent and not different among tissues. The processed guide strand of 21 mer siRNA was observed much more in the cerebrum than in the liver and skeletal muscle (Fig. 4A and B). As shown in Fig. 2C, in contrast, SOD1 mRNA level was relatively lower in the cerebrum in comparison with that in the liver. These clearly indicate that relative ratio of the processed siRNA to the target mRNA in tissues does not explain the difference in siRNA-silencing efficiency.

Next, to examine whether the guide strand of siRNA properly located in the cells, we performed Northern blot analysis after subcellular fractionation of the tissue homogenates. Most of the guide strand was detected in the cytoplasmic fraction in both of the cerebrum and liver (Fig. 4C). These results show that the shRNA is similarly exported from the nucleus to the cytoplasm and that the guide strand should be similarly processed in the cytoplasm in the cerebrum and liver. These suggest that the slicer/RISC function, siRNA-cleaving ability, was lower in the cerebrum than in the liver. Therefore, we finally analyzed expression of Ago2 protein which is considered to be the slicer in mammalian cells [17]. However, the expression of Ago2 protein was not lower in the cerebrum (Fig. 4D), which was previously reported [18,19]. These findings suggest that the lower silencing efficiency in the cerebrum could not be explained by Ago2 level. The exact molecular mechanism

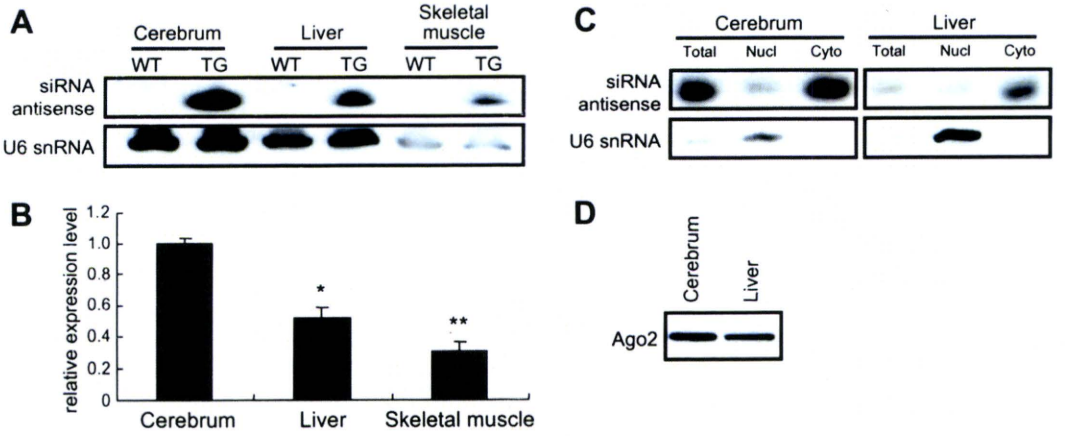

Fig. 4. The processing of shRNA/siRNA in the tissues of the transgenic mice. (A) Detection of siRNA guide strand in the cerebrum, liver and skeletal muscle on Northern blot analysis. (B) Quantification of their band intensity on Northern blot analysis. Values are the ratio to cerebrum (mean and S.D., $n = 3$, $^{*}P < 0.05$, $^{**}P < 0.01$; significance compared to cerebrum). (C) Subcellular localization of the siRNA guide strand in the cerebrum and liver. U6 snRNA is used as a marker of nuclear fraction. (D) Ago2 protein in the cerebrum and liver on Western blot analysis.

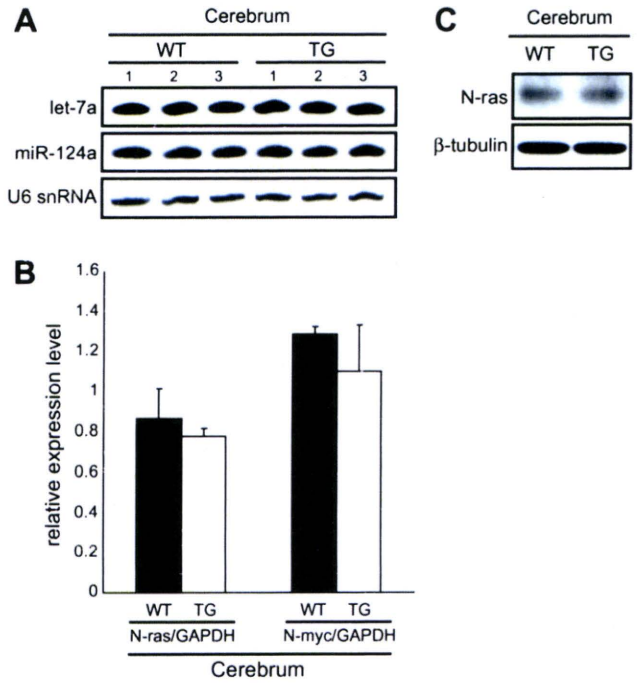

Fig. 5. Endogenous microRNA pathway in the shRNA transgenic mice. (A) Endogenous levels of miRNAs, let-7a (upper) and miR-124a (middle), in the cerebrum on Northern blot analysis. (B) Quantification of N-ras and N-myc levels, which are predicted as target genes of let-7a, in the cerebrum by quantitative RT-PCR (mean and S.D., $n = 3$). (C) N-ras protein in the cerebrum on Western blot analysis.

for the tissue difference in siRNA-silencing efficiency remains to be elucidated.

3.5. Endogenous miRNA pathway is not affected in the cerebrum of shRNA transgenic mice

To analyze whether competition between shRNA and miRNA occurred in the shRNA transgenic mice, we evaluated the expression levels of miRNAs and their target genes in the cerebrum of shRNA transgenic mice. There was no remarkable change in levels of let-7a and miR-124a on Northern blot analysis (Fig. 5A). Expression levels of N-ras and N-myc mRNAs, which were the predicted target genes of let-7a [20,21], were not altered on quantitative RT-PCR (Fig. 5B). Expression level of N-ras protein was not altered on Western blot analysis (Fig. 5C). These results clearly indicate that endogenous miRNA pathway is preserved in the shRNA transgenic mice.

The reproducibility of all results was confirmed by at least two experiments.

4. Discussion

We demonstrated the tissue difference in siRNA-silencing efficiency in the anti-SOD1 shRNA transgenic mice, but could not make clear the exact mechanism for the difference. However, the silencing effects in the tissues were generally good (>80%), and the anti-SOD1 shRNA transgenic mice could recapitulate the phenotype of fatty liver and female infertility as seen in SOD1-null mice [15,16].

Overexpression of shRNA from transgene did not induce apparent adverse effect including inhibition of endogenous miRNA pathway in our transgenic mice. It is of note that abundant shRNA/siRNA exogenously delivered by adeno-associated virus (AAV) vectors can cause drastic toxicity in the liver or brain possibly due to oversaturation of endogenous miRNA pathway [9,22]. The absence of the toxicity in the shRNA transgenic mice is probably due to its lower expression, because such a tissue toxicity is dependent on expression level of shRNA/siRNA [9,22]. Alternatively, there might be a difference in the processing pathways between shRNA expressed from transgenc and that exogenously expressed by viral vector.

In conclusion, even with tissue difference in siRNA-silencing efficiency, endogenous miRNA pathway being well preserved, the transgenic RNAi approach is considered to be a useful method for analysis of gene function in vivo.

Acknowledgements

This work was supported by Grants from the Ministry of Health Labor and Welfare, Japan (#2212065, 2212070), the 21st Century COE Program on Brain Integration and its Disorders to Tokyo Medical and Dental University.

References

[1] Hannon, G.J. (2002) RNA interference. Nature 418, 244–251.
[2] Dykxhoorn, D.M. and Lieberman, J. (2005) The silent revolution: RNA interference as basic biology, research tool, and therapeutic. Annu. Rev. Med. 56, 401–423.
[3] Grimm, D. and Kay, M.A. (2007) Therapeutic application of RNAi: is mRNA targeting finally ready for prime time? J. Clin. Invest. 117, 3633–3641.
[4] Gao, X. and Zhang, P. (2007) Transgenic RNA interference in mice. Physiology 22, 161–166.
[5] Coumoul, X. and Deng, C.X. (2006) RNAi in mice: a promising approach to decipher gene functions in vivo. Biochimie 88, 637–643.
[6] Kunath, T., Gish, G., Lickert, H., Jones, N., Pawson, T. and Rossant, J. (2003) Transgenic RNA interference in ES cell-derived embryos recapitulates a genetic null phenotype. Nat. Biotechnol. 21, 559–561.
[7] Xia, X.G., Zhou, H., Samper, E., Melov, S. and Xu, Z. (2006) Pol II-expressed shRNA knocks down Sod2 gene expression and causes phenotypes of the gene knockout in mice. PLoS Genet. 2, e10.
[8] Rossi, J.J. (2008) Expression strategies for short hairpin RNA interference triggers. Hum. Gene Ther. 19, 313–317.
[9] Grimm, D., Streetz, K.L., Jopling, C.L., Storm, T.A., Pandey, K., Davis, C.R., Marion, P., Salazar, F. and Kay, M.A. (2006) Fatality in mice due to oversaturation of cellular microRNA/short hairpin RNA pathways. Nature 441, 537–541.
[10] Castanotto, D., Sakurai, K., Lingeman, R., Li, H., Shively, L., Aagaard, L., Soifer, H., Gatignol, A., Riggs, A. and Rossi, J.J. (2007) Combinatorial delivery of small interfering RNAs reduces RNAi efficacy by selective incorporation into RISC. Nucleic Acids Res. 35, 5154–5164.
[11] Saito, Y., Yokota, T., Mitani, T., Ito, K., Anzai, M., Miyagishi, M., Taira, K. and Mizusawa, H. (2005) Transgenic small interfering RNA halts amyotrophic lateral sclerosis in a mouse model. J. Biol. Chem. 280, 42826–42830.
[12] Yokota, T., Miyagishi, M., Hino, T., Matsumura, R., Tasinato, A., Urushitani, M., Rao, R.V., Takahashi, R., Bredesen, D.E., Taira, K. and Mizusawa, H. (2004) siRNA-based inhibition specific for mutant SOD1 with single nucleotide alternation in familial ALS, compared with ribozyme and DNA enzyme. Biochem. Biophys. Res. Commun. 314, 283–291.
[13] Ando, Y., Liang, Y., Ishigaki, S., Niwa, J., Jiang, Y., Kobayashi, Y., Yamamoto, M., Doyu, M. and Sobue, G. (2003) Caspase-1 and -3 mRNAs are differentially upregulated in motor neurons and glial cells in mutant SOD1 transgenic mouse spinal cord: a study using laser microdissection and real-time RT-PCR. Neurochem. Res. 28, 839–846.
[14] Tateno, M., Sadakata, H., Tanaka, M., Itohara, S., Shin, R.M., Miura, M., Masuda, M., Aosaki, T., Urushitani, M., Misawa, H. and Takahashi, R. (2004) Calcium-permeable AMPA receptors promote misfolding of mutant SOD1 protein and development of amyotrophic lateral sclerosis in a transgenic mouse model. Hum. Mol. Genet. 13, 2183–2196.
[15] Uchiyama, S., Shimizu, T. and Shirasawa, T. (2006) CuZn-SOD deficiency causes ApoB degradation and induces hepatic lipid accumulation by impaired lipoprotein secretion in mice. J. Biol. Chem. 281, 31713–31719.
[16] Matzuk, M.M., Dionne, L., Guo, Q., Kumar, T.R. and Lebovitz, R.M. (1998) Ovarian function in superoxide dismutase 1 and 2 knockout mice. Endocrinology 139, 4008–4011.
[17] Meister, G., Landthaler, M., Patkaniowska, A., Dorsett, Y., Teng, G. and Tuschl, T. (2004) Human Argonaute2 mediates RNA cleavage targeted by miRNAs and siRNAs. Mol. Cell 15, 185–197.
[18] González-González, E., López-Casas, P.P. and del Mazo, J. (2008) The expression patterns of genes involved in the RNAi pathways are tissue-dependent and differ in the germ and somatic cells of mouse testis. Biochim. Biophys. Acta 1779, 306–311.
[19] Sago, N., Omi, K., Tamura, Y., Kunugi, H., Toyo-oka, T., Tokunaga, K. and Hohjoh, H. (2004) RNAi induction and activation in mammalian muscle cells

where Dicer and eIF2C translation initiation factors are barely expressed. Biochem. Biophys. Res. Commun. 319, 50–57.
[20] Johnson, S.M., Grosshans, H., Shingara, J., Byrom, M., Jarvis, R., Cheng, A., Labourier, E., Reinert, K.L., Brown, D. and Slack, F.J. (2005) RAS is regulated by the let-7 microRNA family. Cell 120, 635–647.
[21] Sampson, V.B., Rong, N.H., Han, J., Yang, Q., Aris, V., Soteropoulos, P., Petrelli, N.J., Dunn, S.P. and Krueger, L.J. (2007) MicroRNA let-7a down-regulates MYC and reverts MYC-induced growth in Burkitt lymphoma cells. Cancer Res. 67, 9762–9770.
[22] McBride, J.L., Boudreau, R.L., Harper, S.Q., Staber, P.D., Monteys, A.M., Martins, I., Gilmore, B.L., Burstein, H., Peluso, R.W., Polisky, B., Carter, B.J. and Davidson, B.L. (2008) Artificial miRNAs mitigate shRNA-mediated toxicity in the brain: implications for the therapeutic development of RNAi. Proc. Natl. Acad. Sci. USA 105, 5868–5873.

HUMAN GENE THERAPY 22:27–34 (January 2011)

DOI: 10.1089/hum.2010.054

Research Articles

In Vivo Application of an RNAi Strategy for the Selective Suppression of a Mutant Allele

Takayuki Kubodera,[1] Hiromi Yamada,[1] Masayuki Anzai,[2] Shinga Ohira,[1] Shigefumi Yokota,[1] Yukihiko Hirai,[3] Hideki Mochizuki,[4] Takashi Shimada,[3] Tasuku Mitani,[2] Hidehiro Mizusawa,[1] and Takanori Yokota[1]

Abstract

Gene therapy for dominantly inherited diseases with small interfering RNA (siRNA) requires mutant allele-specific suppression when genes in which mutation causes disease normally have an important role. We previously proposed a strategy for selective suppression of mutant alleles; both mutant and wild-type alleles are inhibited by most effective siRNA, and wild-type protein is restored using mRNA mutated to be resistant to the siRNA. Here, to prove the principle of this strategy *in vivo*, we applied it to our previously reported anti–copper/zinc superoxide dismutase (SOD1) short hairpin RNA (shRNA) transgenic (Tg) mice, in which the expression of the endogenous wild-type *SOD1* gene was inhibited by more than 80%. These shRNA Tg mice showed hepatic lipid accumulation with mild liver dysfunction due to downregulation of endogenous wild-type SOD1. To rescue this side effect, we generated siRNA-resistant SOD1 Tg mice and crossed them with anti-SOD1 shRNA Tg mice, resulting in the disappearance of lipid accumulation in the liver. Furthermore, we also succeeded in mutant SOD1-specific gene suppression in the liver of $SOD1^{G93A}$ Tg mice, a model for amyotrophic lateral sclerosis, using intravenously administered viral vectors. Our method may prove useful for siRNA-based gene therapy for dominantly inherited diseases.

Introduction

RNA INTERFERENCE (RNAi) is evolutionally conserved sequence-specific post-transcriptional gene silencing mediated by small double-stranded RNA (Elbashir *et al.*, 2001). This post-transcriptional gene silencing can be effectively induced by exogenously introduced small interfering RNA (siRNA) or intracellularly expressed short hairpin RNA (shRNA) in mammalian cells (Dykxhoorn *et al.*, 2006a). The therapeutic efficacy of RNAi on human diseases has been demonstrated in various animal models using either directly delivered siRNA or viral vector-delivered shRNA (Bumcrot *et al.*, 2006; Kim and Rossi, 2007). Among the promising targets for siRNA/shRNA therapy are dominantly inherited diseases in which the aberrant proteins encoded by mutant alleles are eliminated by siRNA/shRNA. In order to test the hypothesis that siRNA-mediated mutant gene silencing is able to ameliorate dominantly inherited diseases, we generated shRNA transgenic (Tg) mice in which shRNA against copper/zinc superoxide dismutase (SOD1) was ubiquitously overexpressed. This mouse demonstrated marked suppression of endogenous *SOD1*, the gene in which mutation causes familial amyotrophic lateral sclerosis (ALS) (Saito *et al.*, 2005; Yokota *et al.*, 2007). When $SOD1^{G93A}$ Tg mice, a model for ALS (Gurney *et al.*, 1994), were crossed with anti-SOD1 shRNA Tg mice, the resultant double Tg mice demonstrated a dramatic delay in the onset and progression of ALS by inhibiting mutant SOD1 production (Saito *et al.*, 2005; Yokota *et al.*, 2007).

A major problem encountered in our strategy to silence the mutant allele with RNAi in $SOD1^{G93A}$ Tg mice was that expressed siRNA failed to specifically recognize the point mutation, resulting in suppression of the wild-type allele in addition to the mutant allele. In order to treat dominantly inherited diseases using this RNAi strategy, mutant allele-specific suppression is necessary, especially when the genes in which mutation causes diseases have normally an important role. Anti-SOD1 shRNA Tg mice that demonstrate marked

[1]Department of Neurology and Neurological Science, Tokyo Medical and Dental University, Bunkyo-ku, Tokyo 113-8519, Japan.
[2]Institute of Advanced Technology, Kinki University, Kainan, Wakayama 642-0017, Japan.
[3]Department of Biochemistry and Molecular Biology, Nippon Medical School, Bunkyo-ku, Tokyo 113-8602, Japan.
[4]Department of Neurology, School of Medicine, Kitasato University, Sagamihara, Kanagawa 252-0374, Japan.

suppression of endogenous wild-type SOD1 also exhibit a fatty liver, similar to that observed in SOD1 knockout mice (Sasaguri *et al.*, 2009). siRNA can be designed to discriminate between single nucleotide alterations by targeting the mutation itself or disease-linked polymorphisms (Gonzalez-Alegre *et al.*, 2003; Miller *et al.*, 2003, 2004; Li *et al.*, 2004; Dykxhoorn *et al.*, 2006b; van Bilsen *et al.*, 2008). In a systematic analysis investigating the design of single nucleotide-specific siRNA, mismatches located in the central and 3′ regions of the guide strand (especially at positions 10 and 16 from the 5′ end) provided a high efficacy of single nucleotide discrimination between mutant and wild-type alleles (Schwarz *et al.*, 2006). Introducing a mismatch into the seed region of siRNA was also shown to enhance discrimination (Ohnishi *et al.*, 2008). We have also reported on the design of siRNA that demonstrates relative discrimination of a mutant allele possibly resulting from a change in the RNA secondary structure (Li *et al.*, 2004).

Despite these design strategies, discrimination of mutant and wild-type alleles is not always complete. In addition, the cleavage efficiency of the mutant allele is not necessarily maximal, as the selection sites used in the design of siRNA are limited to the siRNA-related region. More than 125 different mutations in the *SOD1* gene in familial ALS have been identified to date (Pasinelli and Brown, 2006). We have designed mutant allele-specific siRNA for G93A and A4V SOD1 (Yokota *et al.*, 2004), but not for G37R SOD1. To overcome these problems, we proposed a novel method for allele-specific suppression by siRNA where both mutant and wild-type alleles are inhibited by most effective siRNA and where wild-type protein is restored using wild-type mRNA modified to be resistant to the siRNA. The amino acid sequence encoded by modified mRNA is the same as that of native mRNA, whereas the nucleotide sequence of mRNA targeted by siRNA is altered (Kubodera *et al.*, 2005). A similar method of mutant allele-specific siRNA design was reported by another group in the same year (Xia *et al.*, 2005). Here, we examined this strategy *in vivo* by applying the method to the rescue of the anti-SOD1 shRNA Tg mice phenotype and to the selective suppression of the mutant allele in $SOD1^{G93A}$ Tg mice.

Materials and Methods

Construction of expression vectors

Construction of anti-SOD1 shRNA expression vector has been reported previously (Saito *et al.*, 2005). The shRNA sequence (sense sequence position 536–555, NM_000454) of this vector was common to the siRNA target region in both human and mouse SOD1 mRNA. siRNA-resistant human SOD1 expression vector, in which the human wild-type SOD1 genome is mutated so that it is not cleaved by the anti-SOD1 siRNA but is translated to the same amino acid sequence of native human SOD1, was made by site-directed mutagenesis (Stratagene, La Jolla, CA). The human SOD1 promoter and wild-type SOD1 genomic DNA were kindly provided by Dr. Masashi Aoki.

For recombinant adeno-associated virus (rAAV)-mediated delivery of shRNA targeting SOD1 and siRNA-resistant mouse SOD1 cDNA, the anti-SOD1 shRNA expression cassette containing human U6 promoter (shRNA) or that followed by the siRNA-resistant mouse SOD1 expression cassette containing cytomegalovirus (CMV) promoter (siRNA-resistant) was cloned into the plasmid containing adeno-associated virus (AAV) serotype 2 inverted terminal repeats (pAAV-MCS) (Stratagene). For genome copy titration of rAAV vectors, the human growth hormone poly(A) signal was inserted downstream of the shRNA cassette.

Viral vector production

The rAAV pseudotyped-8 (rAAV-2/8; AAV-2 inverted terminal repeat, AAV-8 viral capsid) vectors were produced using the adenovirus-free triple transfection method (Stratagene). The AAV vector plasmid (pAAV), the packaging plasmid (P5E18-VD2/8; a gift from Dr. James M. Wilson, University of Pennsylvania, Philadelphia, PA), and a helper plasmid (pHelper; Stratagene) were co-transfected into human embryonic kidney 293 cells under calcium phosphate precipitation. At 6 hr after transfection, the culture medium was replaced with fresh medium, and the cells were incubated for 48 hr. The cells were then harvested from the culture dishes and pelleted by centrifugation, resuspended in phosphate-buffered saline (PBS), and subjected to three rounds of freeze–thawing. Cell debris was then pelleted by centrifugation at 1,200 *g* for 15 min. AAV vectors were purified using ammonium sulfate precipitation and iodixanol (Axis-Shield, Norton, MA) continuous gradient centrifugation. Genome titers of the AAV vectors were determined by quantitative polymerase chain reaction (PCR) using the TaqMan system (Taymans *et al.*, 2007). The following primers and probes targeting the poly(A) signal were used: 5′-CAGGCTGGTC TCCAACTCCTC-3′ and 5′-GCAGTGGTTCACGCCTGTAA-3′ served as the primer set, and 5′-TACCCACCTTGGCCTC-3′ served as the probe.

Animals

Animal experiments were performed in accordance with the Guidelines for Animal Experimentation of Tokyo Medical and Dental University and were pre-approved by the local ethics committee (protocol 0090104). The generation of anti-SOD1 siRNA Tg mice has been described previously (Saito *et al.*, 2005). To produce siRNA-resistant human SOD1 Tg mice, the siRNA-resistant human SOD1 expression vector was injected into fertilized mouse eggs. Double Tg mice were generated by crossing anti-SOD1 shRNA Tg mice with siRNA-resistant human SOD1 Tg mice. Genotypes of the mice were determined by PCR analysis using genomic DNA from the tail tip. PCR was carried out using the following primer sets: 5′-CATCAGCCCTAATCCATCTGA-3′ and 5′-CGCGACTAACAATCAAAGTGA-3′ for siRNA-resistant human SOD1 Tg mice and 5′-CTTGGGTAGTTTGCAG-3′ and 5′-CAGGAAACAGCTATGAC-3′ for anti-SOD1 shRNA Tg mice.

AAV injection

$SOD1^{G93A}$ Tg mice were intravenously administered a single dose of 1×10^{12} vector genomes of rAAV2/8-shRNA or -shRNA/resistant SOD1 vectors via the tail vein. All mice were sacrificed 3 weeks post-injection. Mice were deeply anesthetized with pentobarbital sodium and perfused with cold PBS. Tissue samples were then collected and snap-frozen in liquid nitrogen for analysis.

Western blot analysis

Protein samples were extracted from tail, liver, brain, and spinal cord and homogenized in buffer containing 0.1% sodium dodecyl sulfate (SDS), 1% Triton X-100, 1% deoxycholate, and 1 m*M* phenylmethylsulfonyl fluoride. Equal amounts of extracted protein were then mixed with Laemmli sample buffer, denatured, and separated on 15% SDS-polyacrylamide gel electrophoresis. After transfer to a polyvinylidine difluoride membrane (Bio-Rad, Hercules, CA), blots were probed with anti-SOD1 polyclonal antibody S-100 (Assay Designs, Ann Arbor, MI) or anti-β-actin monoclonal antibody (Sigma, St. Louis, MO) and then visualized using enhanced chemiluminescence. Densitometric analysis was performed using Image J application software with the amounts of SOD1 being normalized for β-actin.

Quantitative reverse transcription-PCR

Total RNA was extracted from liver samples using Isogen (Nippon Gene, Tokyo, Japan), and 1 μg of total RNA from each sample was reverse-transcribed to cDNA using the High Capacity RNA-to-cDNA kit (Applied Biosystems, Carlsbad, CA). cDNA was used for quantitative reverse transcription-PCR (qRT-PCR) using the TaqMan system and the ABI Prism 7700 Sequence Detection system (Applied Biosystems) according to the manufacturers' instructions. The following primers and probe were used to quantify mouse and human SOD1: 5′-GGTGCAGGGAACCATCCA-3′ and 5′-CCCATGC TGGCCTTCAGT-3′ for the mouse primer set, with 5′-AGGC AAGCGGTGAACCAGTTGTGTTG-3′ for the mouse probe; and 5′-CCACACCTTCACTGGTCCATTA-3′ and 5′-CGACG GCCCAGTGCA-3′ for the human primer set, with 5′-TTC CTTCTGCTCGAAATTGATGATGCCC-3′ for the human probe.

Measurement of SOD1 activity

Each liver sample was homogenized in 5 volumes (wt/vol) of homogenization buffer containing 0.25 *M* sucrose, 20 m*M* Tris-HCl, and 1 m*M* EDTA and centrifuged at 78,000 *g* for 60 min. The supernatant was carefully removed and analyzed. To inactivate Mn-SOD, the sample was treated with 2% SDS at 37°C for 30 min. After cooling to 4°C, 0.1 volume of 3 *M* KCl was added, and the mixture was centrifuged at 20,000 *g* for 10 min to remove excess SDS. The supernatant was then assayed for SOD activity using the SOD Assay Kit-WST (Dojindo, Kumamoto, Japan) according to the manufacturer's instructions.

Histological study

For histological observation, formalin-fixed, paraffin-embedded liver sections (4 μm thick) were stained with hematoxylin and eosin, and frozen liver sections (8 μm thick) were stained with Sudan III using standard protocols. To quantify hepatic lipid accumulation, the density of lipid droplets (minimal diameter, >2 μm) was measured on the visual fields of a light microscope.

Serum alanine aminotransferase

Blood was collected from the animals via a retro-orbital plexus bleed, and the alanine aminotransferase (ALT) levels in the serum were measured using the ultraviiolet method.

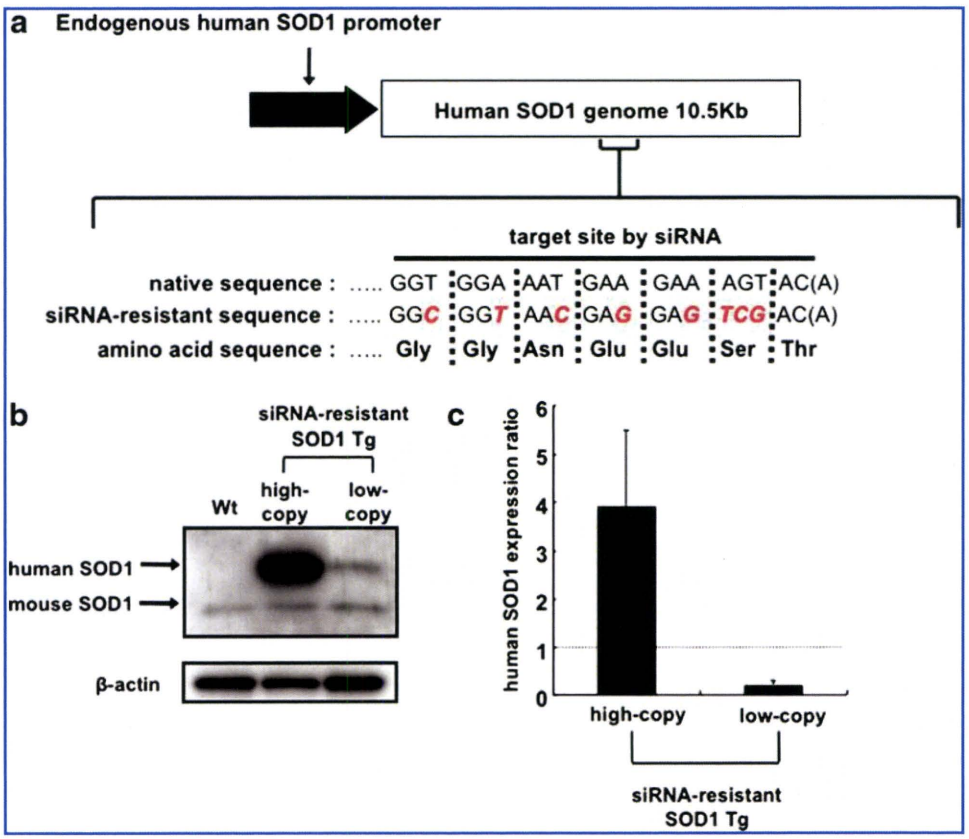

FIG. 1. Generation of siRNA-resistant SOD1 Tg mice. (**a**) Construction of the siRNA-resistant human SOD1 expression vector. The target sequence of anti-SOD1 shRNA is shown below the schematic. The red, italicized letters indicate mutated nucleotides. The amino acid sequence expressed by the siRNA-resistant human SOD1 expression vector is the same as that of the wild-type human SOD1. (**b**) Western blot analysis of SOD1 protein isolated from high-copy and low-copy Tg tails. (**c**) qRT-PCR of human mRNA in the liver. Values are presented as the ratio to endogenous mouse SOD1 mRNA. Data are mean values with SD ($n=3$). Wt, wild-type littermates; high-copy Tg, high-copy siRNA-resistant SOD1 Tg mice; low-copy Tg, low-copy siRNA-resistant SOD1 Tg mice.

Measurements were conducted at Nagahama Life Science Laboratory (Shiga, Japan).

Statistical analysis

Statistical significance was assessed between groups using Student's t test or one-way analysis of variance. Significance was defined as $p < 0.05$.

Results

Generation of siRNA-resistant SOD1 Tg mice

We applied a selective suppression RNAi strategy to rescue the side effects resulting from downregulation of endogenous SOD1 in anti-SOD1 shRNA Tg mice. First, we attempted to generate Tg mice that express wild-type human SOD1 modified to be resistant to the siRNA. The nucleotide sequence

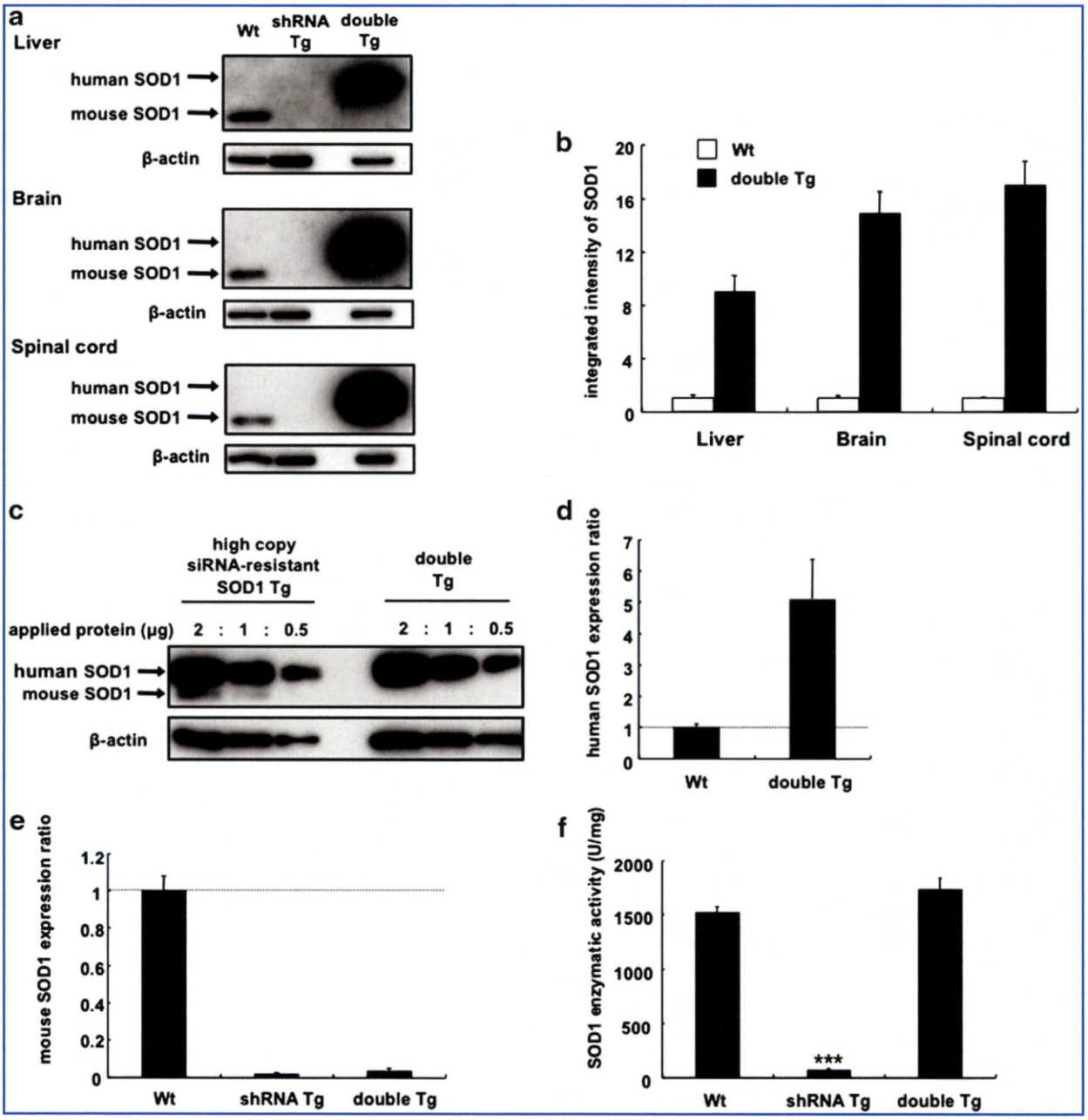

FIG. 2. Restoration of wild-type SOD1 expression in double Tg mice. (**a**) Human SOD1 protein was restored in the liver, brain, and spinal cord of double Tg mice as assessed by western blot analysis. Mouse SOD1 proteins in double Tg mice were reduced as in the anti-SOD1 shRNA Tg mice. (**b**) Corrected densitometry determinations of western blot staining for restored SOD1 protein. Values are presented as the ratio to band intensity of SOD1 protein in wild-type (Wt) littermates. Data are presented as mean values with SD ($n = 3$). (**c**) Human SOD1 protein levels in the liver of high-copy Tg and double Tg mice were similar. (**d**) qRT-PCR of human SOD1 mRNA in the liver. Data are presented as mean values with SD ($n = 3$). (**e**) qRT-PCR of endogenous mouse SOD1 mRNA in double Tg mice. Values are presented as the ratio to endogenous mouse SOD1 mRNA. Data are presented as mean values with SD ($n = 3$). (**f**) SOD1 enzyme activity in the liver. Data are presented as means with SD ($n = 3$ for each group) $^{***}p < 0.001$. shRNA Tg, anti-SOD1 shRNA Tg mice; double Tg, double Tg mice.

encoded by siRNA-resistant SOD1 was altered to encode the same amino acid sequence as that of native SOD1 (Fig. 1a). Two strains of high- and low-copy siRNA-resistant SOD1 Tg mice were obtained in which the expressed human SOD1 protein levels differed on western blot analysis (Fig. 1b). We also quantified the expression of human and mouse SOD1 mRNA by qRT-PCR using TaqMan probes specific for their respective SOD1 mRNA. The expression level of human SOD1 mRNA in low-copy siRNA-resistant SOD1 Tg mice was approximately one-fifth that of endogenous mouse SOD1 mRNA, whereas that in the high-copy siRNA-resistant SOD1 Tg mice was four times higher than that of mouse SOD1 mRNA (Fig. 1c).

Generation of double Tg mice that express both anti-SOD1 shRNA and siRNA-resistant SOD1

We next attempted to generate double Tg mice by crossing high-copy siRNA-resistant SOD1 Tg mice with anti-SOD1 shRNA Tg mice. In the liver, brain, and spinal cord of double Tg mice, human SOD1 protein was robustly expressed, whereas the endogenous mouse SOD1 protein remained suppressed (Fig. 2a). The corrected band density of SOD1 in wild-type littermates and double Tg mice is shown in Fig. 2b. In double Tg mice, the expression level of human SOD1 protein was almost equal to that of siRNA-resistant high-copy SOD1 Tg mice, indicating that human SOD1 was not inhibited by siRNA (Fig. 2c). The expression level of human SOD1 mRNA in double Tg mice was five times higher than that of endogenous mouse SOD1 mRNA observed in wild-type littermates (Fig. 2d), whereas that of mouse SOD1 mRNA was markedly decreased in anti-SOD1 shRNA Tg mice and double Tg mice by 98.0% and 96.1%, respectively (Fig. 2e). In contrast, the enzymatic activity of SOD1 in the liver of double Tg mice was almost equal to that of the wild-type littermates (Fig. 2f).

Rescue of liver dysfunction in double Tg mice

SOD1 is a major antioxidant, and SOD1 knockout mice exhibit abnormalities such as reduced fertility and enhanced susceptibility to axonal injury and cerebral ischemia (Reaume *et al.*, 1996; Matzuk *et al.*, 1998; Kawase *et al.*, 1999). Furthermore, hepatic lipid accumulation has also been found in SOD1 knockout mice (Uchiyama *et al.*, 2006). Thus, it was considered that oxidative stress enhanced hepatic lipid accumulation by impairing lipoprotein secretion due to the degradation of apolipoprotein B in hepatocytes. Similarly, we observed a significant increase in ALT (Fig. 3a) and the presence of numerous small lipid droplets in the liver of anti-SOD1 shRNA Tg mice (Fig. 3b and c).

In double Tg mice, serum ALT levels were recovered to within the normal range (Fig. 3a). Moreover, the number of lipid droplets in the liver of double Tg mice was decreased to levels similar to that of the wild-type mice as observed on Sudan III staining (Fig. 3b and c). The liver abnormalities identified in anti-SOD1 shRNA Tg mice disappeared in double Tg mice, indicating that loss of wild-type SOD1 function was recovered by the expression of siRNA-resistant SOD1.

Vector-mediated delivery of both anti-SOD1 shRNA and siRNA-resistant SOD1

To achieve conditional *in vivo* knockdown of the target gene with this strategy, we used vector-mediated delivery

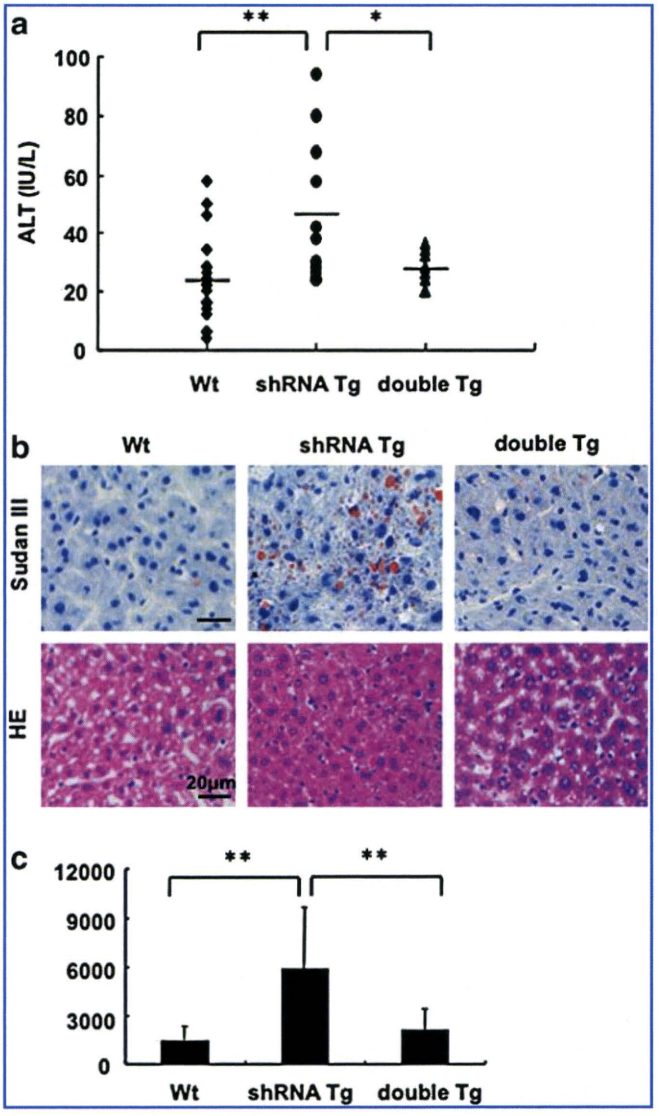

FIG. 3. Disappearance of liver dysfunction in double Tg mice. (**a**) ALT levels in the serum ($n = 20$ for wild-type [Wt] littermates, $n = 11$ for anti-SOD1 shRNA Tg mice, $n = 8$ for double Tg mice). Horizontal bars indicate the mean values. $^{*}p < 0.05$, $^{**}p < 0.01$. (**b**) Histological analysis of the liver. Sections were stained with Sudan III (**upper panel**) and hematoxylin and eosin (HE) (**lower panel**). Scale bar = 20 μm. (**c**) Average number of lipid droplets (>2 μm). Data are presented as mean values with SD. $^{**}p < 0.01$.

with rAAV. In order to introduce both shRNA and siRNA-resistant mRNA to each cell *in vivo*, we generated a construct that dually expressed anti-SOD1 shRNA and siRNA-resistant SOD1 cDNA (pAAV-shRNA/resistant SOD1), as well as shRNA against SOD1 alone (pAAV-shRNA) (Fig. 4a).

$SOD1^{G93A}$ Tg mice were intravenously injected with 1×10^{12} vector genomes per mouse of rAAV-2/8-shRNA or -shRNA/resistant SOD1. Three weeks later, we found that the $SOD1^{G93A}$ Tg mice injected with rAAV-2/8-shRNA demonstrated significant inhibition of both mutant G93A SOD1 and endogenous mouse SOD1 proteins in the liver as assessed by western blot analysis. On the other hand, in $SOD1^{G93A}$ Tg mice injected with rAAV-2/8-shRNA/resistant SOD1, levels

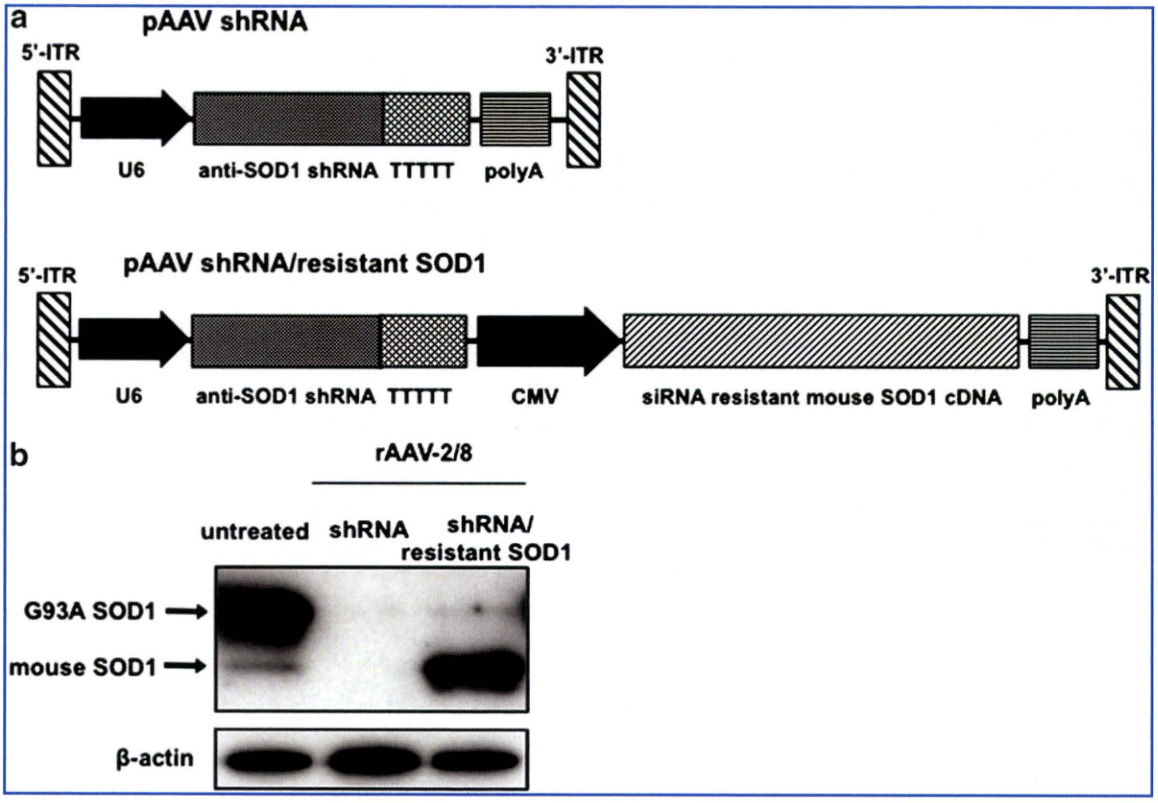

FIG. 4. Vector-mediated delivery of anti-SOD1 shRNA and siRNA-resistant SOD1 cDNA. (**a**) Schematic of constructs packaged in rAAV-2/8 expressing anti-SOD1 shRNA (pAAV shRNA) or co-expressing anti-SOD1 shRNA and siRNA-resistant mouse SOD1 cDNA (pAAV shRNA/resistant SOD1). ITR, inverted terminal repeats. (**b**) Effects of rAAV-2/8 in the liver of SOD1G93A Tg mice assessed by western blot analysis. rAAV-2/8-shRNA or -shRNA/resistant SOD1 was injected into SOD1G93A Tg mice via the tail vein. The mutant G93A SOD1 protein level was reduced, but the wild-type mouse SOD1 protein level was restored in mice treated with the rAAV-2/8-shRNA/resistant SOD1.

of wild-type mouse SOD1 protein were much increased under inhibition of mutant G93A SOD1 protein (Fig. 4b).

Discussion

Our initial reports on our RNAi strategy raised several problems, including (1) the requirement of both siRNA and restored wild-type protein to be delivered to every cell, (2) differences in function that may exist between the endogenous and exogenously expressed proteins, and (3) the control of expression levels of the restored wild-type protein (Kubodera *et al.*, 2005).

In order to express both siRNA and restored wild-type protein in each cell, we constructed a cassette that dually expressed anti-SOD1 shRNA containing U6 promoter and siRNA-resistant wild-type SOD1 cDNA containing CMV promoter in rAAV vectors. Following systemic intravenous injection of this rAAV vector into SOD1^{G93A} Tg mice, mutant G93A SOD1 protein in the liver almost disappeared as seen in mice injected with rAAV vectors expressing anti-SOD1 shRNA alone. In addition, the wild-type mouse SOD1 protein was also restored. As both promoters work ubiquitously, two transcripts should be expressed in each cell. Recently, another vector construct that simultaneously expressed transgene and shRNA was reported (Samakoglu *et al.*, 2006). In this construct, a promoter-less lariat-embedded shRNA sequence was inserted within the intron of the *Pol*II-driven protein-coding transgene, generating efficient shRNA from the processed primary transcript.

In the double transgenic mice, the enzymatic activity of restored siRNA-resistant SOD1 was similar to its endogenous levels, and the side effects observed in the anti-SOD1 shRNA Tg mice disappeared without any other additional side effects. Therefore, the expression level of restored siRNA-resistant SOD1 appeared appropriate for our purpose. However, the level of the restored SOD1 enzymatic activity was much less than expected compared with the overexpressed siRNA-resistant SOD1 mRNA in the double Tg mice. As SOD1 functions in its dimeric form, chimeric dimerization of human and mouse SOD1 may not function as a mouse homodimer. Alternatively, there may be differences in post-translational modifications between recombinant human and endogenous mouse SOD1 in the mouse liver that affects enzymatic activity.

Using rAAV-mediated gene delivery, the protein level of overexpressed wild-type mouse SOD1 in the liver was much greater than the endogenous level. It has been reported that human wild-type SOD1 transgenic mice, unlike mutant SOD1 transgenic mice, do not develop motor abnormalities and paralysis (Gurney *et al.*, 1994; Ripps *et al.*, 1995), while aged mice overexpressing wild-type SOD1 show minor motor abnormalities (Jaarsma *et al.*, 2000). In addition, increased wild-type SOD1 accelerates the phenotype of an ALS mouse model with mutant SOD1 (Deng *et al.*, 2006; Wang *et al.*, 2009).

α-Synuclein, amyloid precursor protein, and peripheral myelin protein-22 are known to cause autosomal dominant disease in the presence of duplication or triplication of a gene locus (Harding, 1995; Singleton *et al.*, 2003; Rovelet-Lecrux *et al.*, 2006), indicating that wild-type protein expression levels should be strictly controlled. The inducible expression system represents one of the possible techniques that can be used to regulate gene expression. A few gene expression systems that can be regulated with a steroid hormone-dependent and tetracycline-dependent transcriptional switch have been reported (Goverdhana *et al.*, 2005; Manfredsson *et al.*, 2009). However, a precise method for tuning the levels of proteins expressed from transgene has not been established.

The major targets of our RNAi strategy are dominantly inherited diseases in which the causative gene normally plays an important role. Recent studies have indicated that mutations in several dominantly inherited diseases, including polyglutamine diseases, prion disease, and Alzheimer's disease, contributed to pathology through both a loss- and gain-of-function (Van Raamsdonk *et al.*, 2005; Harris and True, 2006; Thomas *et al.*, 2006; Shen and Kelleher, 2007; Lim *et al.*, 2008). For example, in the case of spinocerebellar ataxia type 1, which is one of the polyglutamine diseases and caused by the expansion of a glutamine-encoding CAG repeat in the *ataxin-1* gene, ataxin-1 protein forms at least two distinct native complexes. Polyglutamine expansion alters the proportion of the mutant protein participating in the formation of these complexes. One complex then causes disease via a gain-of-function mechanism, whereas the other complex concomitantly causes a loss-of-function (Lim *et al.*, 2008). Our RNAi strategy for allele-specific suppression is suitable for these cases, as concomitant loss of wild-type protein function can be restored in addition to inhibiting the toxicity of the mutant protein. The optimal restored level of the wild-type protein, however, may differ depending on the mechanism of concomitant loss-of-function in each disease.

In conclusion, we present an efficiency of our RNAi strategy for allele-specific suppression *in vivo*, by preventing the side effects due to downregulation of endogenous wild-type protein using Tg mice and furthermore by the mutant allele-specific gene suppression using intravenously administered viral vectors. Although the restored protein level should be specifically determined for each disease, our *in vivo* results indicate that our RNAi strategy is promising for gene therapy of dominantly inherited diseases, especially those exhibiting concomitant loss of wild-type protein function.

Acknowledgments

We thank Dr. Masashi Aoki for providing human SOD1 promoter and cDNA and Dr. James M. Wilson for providing the AAV packaging plasmid. This work was supported in part by grants from the Ministry of Education, Science, Culture, Sports, and Technology, Japan (18659256 and 20790610), the Ministry of Health Labor and Welfare, Japan (2212065), and the 21st Century COE Program on Brain Integration and its Disorders from Tokyo Medical and Dental University.

Author Disclosure Statement

No competing financial interests exist.

References

Bumcrot, D., Manoharan, M., Koteliansky, V., and Sah, D.W. (2006). RNAi therapeutics: A potential new class of pharmaceutical drugs. Nat. Chem. Biol. 2, 711–719.

Deng, H.X., Shi, Y., Furukawa, Y., Zhai, H., Fu, R., Liu, E., Gorrie, G.H., Khan, M.S., Hung, W.Y., Bigio, E.H., Lukas, T., Dal Canto, M.C., O'Halloran, T.V., and Siddique, T. (2006). Conversion to the amyotrophic lateral sclerosis phenotype is associated with intermolecular linked insoluble aggregates of SOD1 in mitochondria. Proc. Natl. Acad. Sci. U.S.A. 103, 7142–7147.

Dykxhoorn, D.M., Palliser, D., and Lieberman, J. (2006a). The silent treatment: siRNAs as small molecule drugs. Gene Ther. 13, 541–552.

Dykxhoorn, D.M., Schlehuber, L.D., London, I.M., and Lieberman, J. (2006b). Determinants of specific RNA interference-mediated silencing of human beta-globin alleles differing by a single nucleotide polymorphism. Proc. Natl. Acad. Sci. U.S.A. 103, 5953–5958.

Elbashir, S.M., Harborth, J., Lendeckel, W., Yalcin, A., Weber, K., and Tuschl, T. (2001). Duplexes of 21-nucleotide RNAs mediate RNA interference in cultured mammalian cells. Nature 411, 494–498.

Gonzalez-Alegre, P., Miller, V.M., Davidson, B.L., and Paulson, H.L. (2003). Toward therapy for DYT1 dystonia: Allele-specific silencing of mutant TorsinA. Ann. Neurol. 53, 781–787.

Goverdhana, S., Puntel, M., Xiong, W., Zirger, J.M., Barcia, C., Curtin, J.F., Soffer, E.B., Mondkar, S., King, G.D., Hu, J., Sciascia, S.A., Candolfi, M., Greengold, D.S., Lowenstein, P.R., and Castro, M.G. (2005). Regulatable gene expression systems for gene therapy applications: Progress and future challenges. Mol. Ther. 12, 189–211.

Gurney, M.E., Pu, H., Chiu, A.Y., Dal Canto, M.C., Polchow, C.Y., Alexander, D.D., Caliendo, J., Hemtati, A., Kwon, Y.W., Deng, H.X., Chen, W., Zhai, P., Sufit, R.L., and Siddique, T. (1994). Motor neuron degeneration in mice that express a human Cu,Zn superoxide dismutase mutation. Science 264, 1772–1775.

Harding, A.E. (1995). From the syndrome of Charcot, Marie and Tooth to disorders of peripheral myelin proteins. Brain 118, 809–818.

Harris, D.A., and True, H.L. (2006). New insights into prion structure and toxicity. Neuron 50, 353–357.

Jaarsma, D., Haasdijk, E.D., Grashorn, J.A., Hawkins, R., Van Duijn, W., Verspaget, H.W., London, J., and Holstege, J.C. (2000). Human Cu/Zn superoxide dismutase (SOD1) overexpression in mice causes mitochondrial vacuolization, axonal degeneration, and premature motoneuron death and accelerates motoneuron disease in mice expressing a familial amyotrophic lateral sclerosis mutant SOD1. Neurobiol. Dis. 7, 623–643.

Kawase, M., Murakami, K., Fujimura, M., Morita-Fujimura, Y., Gasche, Y., Kondo, T., Scott, R.W., and Chan, P.H. (1999). Exacerbation of delayed cell injury after transient global ischemia in mutant mice with CuZn superoxide dismutase deficiency. Stroke 30, 1962–1968.

Kim, D.H., and Rossi, J.J. (2007). Strategies for silencing human disease using RNA interference. Nat. Rev. Genet. 8, 173–184.

Kubodera, T., Yokota, T., Ishikawa, K., and Mizusawa, H. (2005). New RNAi strategy for selective suppression of a mutant allele in polyglutamine disease. Oligonucleotides 15, 298–302.

Li, Y., Yokota, T., Matsumura, R., Taira, K., and Mizusawa, H. (2004). Sequence-dependent and independent inhibition specific for mutant ataxin-3 by small interfering RNA. Ann. Neurol. 56, 124–129.

Lim, J., Crespo-Barreto, J., Jafar-Nejad, P., Bowman, A.B., Richman, R., Hill, D.E., Orr, H.T., and Zoghbi, H.Y. (2008).

Opposing effects of polyglutamine expansion on native protein complexes contribute to SCA1. Nature 452, 713–718.

Manfredsson, F.P., Burger, C., Rising, A.C., Zuobi-Hasona, K., Sullivan, L.F., Lewin, A.S., Huang, J., Piercefield, E., Muzyczka, N., and Mandel, R.J. (2009). Tight long-term dynamic doxycycline responsive nigrostriatal GDNF using a single rAAV vector. Mol. Ther. 17, 1857–1867.

Matzuk, M.M., Dionne, L., Guo, Q., Kumar, T.R., and Lebovitz, R.M. (1998). Ovarian function in superoxide dismutase 1 and 2 knockout mice. Endocrinology 139, 4008–4011.

Miller, V.M., Xia, H., Marrs, G.L., Gouvion, C.M., Lee, G., Davidson, B.L., and Paulson, H.L. (2003). Allele-specific silencing of dominant disease genes. Proc. Natl. Acad. Sci. U.S.A. 100, 7195–7200.

Miller, V.M., Gouvion, C.M., Davidson, B.L., and Paulson, H.L. (2004). Targeting Alzheimer's disease genes with RNA interference: An efficient strategy for silencing mutant alleles. Nucleic Acids Res. 32, 661–668.

Ohnishi, Y., Tamura, Y., Yoshida, M., Tokunaga, K., and Hohjoh, H. (2008). Enhancement of allele discrimination by introduction of nucleotide mismatches into siRNA in allele-specific gene silencing by RNAi. PLoS ONE 3, e2248.

Pasinelli, P., and Brown, R.H. (2006). Molecular biology of amyotrophic lateral sclerosis: Insights from genetics. Nat. Rev. Neurosci. 7, 710–723.

Reaume, A.G., Elliott, J.L., Hoffman, E.K., Kowall, N.W., Ferrante, R.J., Siwek, D.F., Wilcox, H.M., Flood, D.G., Beal, M.F., Brown, R.H., Jr., Scott, R.W., and Snider, W.D. (1996). Motor neurons in Cu/Zn superoxide dismutase-deficient mice develop normally but exhibit enhanced cell death after axonal injury. Nat. Genet. 13, 43–47.

Ripps, M.E., Huntley, G.W., Hof, P.R., Morrison, J.H., and Gordon, J.W. (1995). Transgenic mice expressing an altered murine superoxide dismutase gene provide an animal model of amyotrophic lateral sclerosis. Proc. Natl. Acad. Sci. U.S.A. 92, 689–693.

Rovelet-Lecrux, A., Hannequin, D., Raux, G., Le Meur, N., Laquerriere, A., Vital, A., Dumanchin, C., Feuillette, S., Brice, A., Vercelletto, M., Dubas, F., Frebourg, T., and Campion, D. (2006). APP locus duplication causes autosomal dominant early-onset Alzheimer disease with cerebral amyloid angiopathy. Nat. Genet. 38, 24–26.

Saito, Y., Yokota, T., Mitani, T., Ito, K., Anzai, M., Miyagishi, M., Taira, K., and Mizusawa, H. (2005). Transgenic small interfering RNA halts amyotrophic lateral sclerosis in a mouse model. J. Biol. Chem. 280, 42826–42830.

Samakoglu, S., Lisowski, L., Budak-Alpdogan, T., Usachenko, Y., Acuto, S., Di Marzo, R., Maggio, A., Zhu, P., Tisdale, J.F., Riviere, I., and Sadelain, M. (2006). A genetic strategy to treat sickle cell anemia by coregulating globin transgene expression and RNA interference. Nat. Biotechnol. 24, 89–94.

Sasaguri, H., Mitani, T., Anzai, M., Kubodera, T., Saito, Y., Yamada, H., Mizusawa, H., and Yokota, T. (2009). Silencing efficiency differs among tissues and endogenous microRNA pathway is preserved in short hairpin RNA transgenic mice. FEBS Lett. 583, 213–218.

Schwarz, D.S., Ding, H., Kennington, L., Moore, J.T., Schelter, J., Burchard, J., Linsley, P.S., Aronin, N., Xu, Z., and Zamore, P.D. (2006). Designing siRNA that distinguish between genes that differ by a single nucleotide. PLoS Genet. 2, e140.

Shen, J., and Kelleher, R.J., 3rd (2007). The presenilin hypothesis of Alzheimer's disease: Evidence for a loss-of-function pathogenic mechanism. Proc. Natl. Acad. Sci. U.S.A. 104, 403–409.

Singleton, A.B., Farrer, M., Johnson, J., Singleton, A., Hague, S., Kachergus, J., Hulihan, M., Peuralinna, T., Dutra, A., Nussbaum, R., Lincoln, S., Crawley, A., Hanson, M., Maraganore, D., Adler, C., Cookson, M.R., Muenter, M., Baptista, M., Miller, D., Blancato, J., Hardy, J., and Gwinn-Hardy, K. (2003). alpha-Synuclein locus triplication causes Parkinson's disease. Science 302, 841.

Taymans, J.M., Vandenberghe, L.H., Haute, C.V., Thiry, I., Deroose, C.M., Moretelmans, L., Wilson, J.M., Debyser, Z., and Baekelandt, V. (2007). Comparative analysis of adeno-associated viral vector serotypes 1, 2, 5, 7, and 8 in mouse brain. Hum. Gene Ther. 18, 195–206.

Thomas, P.S., Jr., Fraley, G.S., Damian, V., Woodke, L.B., Zapata, F., Sophier, B.L., Plymate, S.R., and La Spada, A.R. (2006). Loss of endogenous androgen receptor protein accelerates motor neuron degeneration and accentuates androgen insensitivity in a mouse model of X-linked spinal and bulbar muscular atrophy. Hum. Mol. Genet. 15, 2225–2238.

Uchiyama, S., Shimizu, T., and Shirasawa, T. (2006). CuZn-SOD deficiency causes ApoB degradation and induces hepatic lipid accumulation by impaired lipoprotein secretion in mice. J. Biol. Chem. 281, 31713–31719.

van Bilsen, P.H., Jaspers, L., Lombardi, M.S., Odekerken, J.C., Burright, E.N., and Kaemmerer, W.F. (2008). Identification and allele-specific silencing of the mutant huntingtin allele in Huntington's disease patient-derived fibroblasts. Hum. Gene Ther. 19, 710–719.

Van Raamsdonk, J.M., Pearson, J., Rogers, D.A., Bissada, N., Vogl, A.W., Hayden, M.R., and Leavitt, B.R. (2005). Loss of wild-type huntingtin influences motor dysfunction and survival in the YAC128 mouse model of Huntington disease. Hum. Mol. Genet. 14, 1379–1392.

Wang, L., Deng, H.X., Grisotti, G., Zhai, H., Siddique, T., and Roos, R.P. (2009). Wild-type SOD1 overexpression accelerates disease onset of a G85R SOD1 mouse. Hum. Mol. Genet. 18, 1642–1651.

Xia, X.G., Zhou, H., Zhou, S., Yu, Y., Wu, R., and Xu, Z. (2005). An RNAi strategy for treatment of amyotrophic lateral sclerosis caused by mutant Cu,Zn superoxide dismutase. J. Neurochem. 92, 362–367.

Yokota, T., Miyagishi, M., Hino, T., Matsumura, R., Tasinato, A., Urushitani, M., Rao, R.V., Takahashi, R., Bredesen, D.E., Taira, K., and Mizusawa, H. (2004). siRNA-based inhibition specific for mutant SOD1 with single nucleotide alternation in familial ALS, compared with ribozyme and DNA enzyme. Biochem. Biophys. Res. Commun. 314, 283–291.

Yokota, T., Sasaguri, H., Saito, Y., Yamada, H., Unno, T., Yamamoto, Y., Kubodera, T., Anzai, M., Mitani, T., and Mizusawa, H. (2007). Increase of disease duration of amyotrophic lateral sclerosis in a mouse model by transgenic small interfering RNA. Arch. Neurol. 64, 145–146.

Address correspondence to:
Dr. Takanori Yokota
Department of Neurology and Neurological Science
Tokyo Medical and Dental University
1-5-45 Yushima, Bunkyo-ku, Tokyo 113-8519, Japan

E-mail: tak-yokota.nuro@tmd.ac.jp

Received for publication March 14, 2010;
accepted after revision July 19, 2010.

Published online: July 20, 2010.

Biochemical and Biophysical Research Communications 405 (2011) 204–209

Contents lists available at ScienceDirect

Biochemical and Biophysical Research Communications

journal homepage: www.elsevier.com/locate/ybbrc

Intraperitoneal AAV9-shRNA inhibits target expression in neonatal skeletal and cardiac muscles

Azat Mayra [a], Hiroyuki Tomimitsu [a], Takayuki Kubodera [a], Masaki Kobayashi [a], Wenying Piao [a], Fumiko Sunaga [a], Yukihiko Hirai [b], Takashi Shimada [b], Hidehiro Mizusawa [a], Takanori Yokota [a,*]

[a] Department of Neurology and Neurological Science, Graduate School, Tokyo Medical and Dental University, 1-5-45 Yushima, Bunkyo-ku, Tokyo 113-8519, Japan
[b] Department of Biochemistry and Molecular Biology, Nippon Medical School, 1-1-5 Sendagi, Bunkyo-ku, Tokyo 113-8602, Japan

ARTICLE INFO

Article history:
Received 24 November 2010
Available online 8 January 2011

Keywords:
shRNA
AAV9
Neonatal

ABSTRACT

Systemic injections of AAV vectors generally transduce to the liver more effectively than to cardiac and skeletal muscles. The short hairpin RNA (shRNA)-expressing AAV9 (shRNA-AAV9) can also reduce target gene expression in the liver, but not enough in cardiac or skeletal muscles. Higher doses of shRNA-AAV9 required for inhibiting target genes in cardiac and skeletal muscles often results in shRNA-related toxicity including microRNA oversaturation that can induce fetal liver failure.

In this study, we injected high-dose shRNA-AAV9 to neonates and efficiently silenced genes in cardiac and skeletal muscles without inducing liver toxicity. This is because AAV is most likely diluted or degraded in the liver than in cardiac or skeletal muscle during cell division after birth. We report that this systemically injected shRNA-AAV method does not induce any major side effects, such as liver dysfunction, and the dose of shRNA-AAV is sufficient for gene silencing in skeletal and cardiac muscle tissues. This novel method may be useful for generating gene knockdown in skeletal and cardiac mouse tissues, thus providing mouse models useful for analyzing diseases caused by loss-of-function of target genes.

1. Introduction

Since the discovery that RNA interference (RNAi), mediated by small interference RNA (siRNA), can inhibit target gene expression, RNAi has become the standard tool for sequence-specific knockdown of gene expression in molecular biology [1]. RNAi biology utilizes short hairpin RNA (shRNA) usually expressed from plasmid or viral vectors. Base-pair stems and a loop region characterize shRNAs. Different types of promoters can be used for shRNA expression and, therefore, various knockdown models using tissue- or cell-specific promoters for target genes can be generated [2].

Another small RNA, microRNA (miRNA), is known to bind endogenous non-protein coding genes, with the precursors of miRNAs being hairpin structures similar to shRNAs. The miRNA and shRNA are known to utilize the common pathways of exportin-5 for nuclear export and the processing by Dicer and Argonaute family proteins in the cytoplasm. As these processes are competed for by miRNA and shRNA, a high level of shRNA expression could interfere with miRNA maturation and cause damage to the cells [1,4]. From these view points, properly designed and expressed shRNAs are necessary to establish knockdown models of chronic diseases that are both acquired and inherited.

For generating in vivo models of disease by using shRNAs, the main constraint is the difficulty in delivering the shRNA to the target tissues. Delivery of gene vectors to local skeletal muscles and cardiac muscle has been achieved by direct intramuscular injection or by local blood perfusion with nonviral and viral vectors, including plasmid DNA and adeno-associated virus (AAV) [5,6]. A number of AAV serotype vectors are available, with AAV1, 6, 8 and 9 being reported to efficiently express the transgenes in skeletal and cardiac muscles [7–11]. However, there are only a few reports claiming that systemic AAV-shRNA vector injection can significantly inhibit target genes in skeletal muscle. One paper showed a significant reduction of the target gene in skeletal muscle and liver by using tail vein injection of AAV type 6 [12], yet liver function was not examined. In our preliminary study, intravenously administered high dose AAV8- or AAV9-shRNA (1×10^{12} v.g./mouse) achieved substantial inhibition of the target gene in the liver, but induced severe liver damage without sufficient gene silencing in the skeletal muscle itself. Intraperitoneal administration of AAV vectors in neonatal mice showed significantly higher expression of target genes than in adult mice. Moreover, using systemic administration of AAV vectors in neonatal mice, target genes can be delivered to neurons and cardiac and skeletal muscle more efficiently [10,13–16]. In this study, we injected AAV9-shRNA intraperitoneally to neonates and sufficiently inhibited the target genes in skeletal and cardiac muscles without detecting any side effects, including liver damage.

* Corresponding author. Fax: +81 3 5803 0169.
E-mail address: tak-yokota.nuro@tmd.ac.jp (T. Yokota).

0006-291X/$ - see front matter © 2011 Elsevier Inc. All rights reserved.
doi:10.1016/j.bbrc.2011.01.009

2. Materials and methods

2.1. Construction of the anti-SOD1 shRNA AAV9 vector

We prepared the anti-SOD1 shRNA cassette as previously reported [17]. The anti-SOD1 shRNA cassette was cloned downstream of the polymerase III (PolIII) human U6 promoter in the AAV vector (Stratagene, La Jolla, CA, USA) plasmid (Fig. 1). The silencing efficiency of the anti-SOD1 shRNA sequence was verified using several cultured cell lines and transgenic mice expressing the anti-SOD1 shRNA, as previously described [3]. Human growth hormone polyadenylation (hGH poly A) cassette (Stratagene) was inserted downstream of the shRNA sequence in the vector for the titration assay of the vector by quantitative real-time PCR (Fig. 1).

2.2. Production and titration of the anti-SOD-shRNA AAV9 vector

The recombinant viral vector was produced according to the three-plasmid transfection protocol using the calcium phosphate method [18]. Human embryonic kidney cultured cells (HEK 293 cells) at approximately 70% confluence were transfected with the AAV9 packaging plasmid, pRep2/Cap9 (a kind gift from Wilson J), adenovirus Helper plasmid (Stratagene), and the pAAV-anti-SOD1-shRNA plasmid, at a ratio of 1:1:1. At 6 h post-transfection the medium was replaced with fresh culture medium containing 2% fetal bovine serum (Sigma, St. Louis, MO, USA), and the cells were cultured for 48 h at 37 °C. After the incubation, the cells were harvested and pelleted by centrifugation at 4000 rpm. The pellets were then resuspended in Tris–HCl (pH 8.5), and after treatment with 5% sodium deoxycholate for 30 min at 37 °C, the cells were subjected to three freeze–thaw cycles. The cell suspension was treated with Benzonase (Merck, Darmstadt, Denmark), followed by the process of ammonium sulfate deposition using $(NH_4)_2SO_4$ (pH 8.5). Cell pellets contained the AAV dissolved in phosphate buffered saline (PBS), and the viral solution was layered with Optiprep (Axis-shield, Oslo, Norway). After centrifugation of the solution at 52,000 rpm for 17 h at 15 °C, the viral fractions were collected from the bottom of the gradient.

Genome titers of the AAV vectors were determined by quantitative PCR using the TaqMan system. The following primers and probes targeting the polyA signal were used: 5′-CAGGCTGGTC TCCAACTCCTC-3′ and 5′-GCAGTGGTTCACGCCTGTAA-3′ served as the primer set, and 5′-TACCCACCTTGGCCTC-3′ served as the probe.

2.3. Animals

All of the animal procedures were performed in accordance with the protocols approved by the Animal Experiment Committee of Tokyo Medical and Dental University (#0100101). All of the ICR mice were obtained from Orient Yeast Co. Ltd. (Tokyo, Japan). Postnatal day-1 ICR mice were injected intraperitoneally with 5×10^{11} vector genome per gram (v.g./g) of the anti-SOD1 shRNA AAV9 vector ($n = 4$). Non-injected littermates were used as the control group ($n = 4$). The body weights of the mice were measured chronologically. At 4 weeks after the injection, all of the mice were euthanized after performing the rotarod tests. Blood, skeletal muscles (quadriceps and hamstrings), cardiac muscle, and liver tissues were collected for analysis.

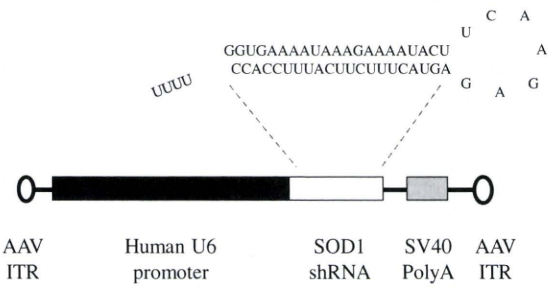

Fig. 1. Construction of the anti-SOD1 shRNA AAV9 vector. The anti-SOD1 shRNA expression AAV9 vector including an anti-SOD1 shRNA between the polymerase III human U6 promoter and hGH polyA cassette.

2.4. Rotarod test

The rotarod test was performed using the accelerating Rotarod (Ugo Basile Biological Research Apparatus, Varese, Italy). The 4-week-old mice in both groups were placed on the rod (3 cm diameter) in four trials each day, for a series of 4 days. Each trial lasted up to a maximum of 10 min; the time spent on the rod without falling was recorded. The average time of each group was calculated and statistical significance was assessed by one-way ANOVA. Significance was defined as $p < 0.05$.

2.5. Northern blotting analysis of shRNA

The RNAs were derived from quadriceps, hamstrings, cardiac muscle, and liver using MirVana (Ambion, Austin, TX, USA). Three micrograms of RNA derived from each tissue were separated on 18% polyacrylamide-urea gels, and transferred to Hybond-N+ membranes (GE Healthcare, Piscataway, UK). The blots were hybridized with a probe against the antisense sequence of the shRNA. The probe sequence was 5′-GGTGGAAATGAAGAAAGTAC-3′. The probe was labeled using DIG Oligonucleotide 3′-End Labeling Kit 2nd Generation (Roche, Penzberg, Germany). The signal was visualized using the Gene Images CDP-star detection kit (GE Healthcare).

2.6. Measurement of RNA reduction by quantitative RT-PCR

Total RNAs were extracted from the collected tissues using Isogen (Nippon Gene, Toyama, Japan). DNase-treated total RNAs (0.5 μg) were reverse transcribed using SuperScript III Reverse Transcriptase (Invitrogen, Carlsbad, CA, USA). The cDNAs were amplified by the quantitative TaqMan system on a Light Cycle 480 Real-Time PCR Instrument (Roche), according to the manufacturer's protocol. SOD1 mRNA expression level in each tissue was measured using the primers and probe designed as follows: Forward primer: 5′-GGTGCAGGGAACCATCCA-3′, reverse primer: 5′-CCCATGCTGGCCTTCAGT-3′, and the probe: 5′-AGGCAAGCGGTGAA CCAGTTGTGTTG-3′. In order to normalize the RT-PCR values, the cDNAs were also amplified quantitatively with the TaqMan primers and the probe sets for GAPDH (Applied Biosystems, Warrington, UK). The ratio of SOD1 mRNA expression level to GAPDH expression was calculated to estimate the shRNA silencing efficiency. Significant differences between the two groups were calculated with the Welch's *T*-test.

2.7. Western blotting

Protein samples were extracted from the liver, hamstrings and cardiac muscles. The tissues were homogenized in cold homogenization buffer containing 0.1% sodium dodecylsulfate (SDS), 1% sodium deoxycholate, 1% Triton X-100, and 1 mM phenylmethylsulfonyl fluoride, together with a protein inhibitor cocktail (Roche). Eight micrograms of the extracted protein of each sample was mixed with laemmli sample buffer (BioRad, Hercules, CA, USA), denatured at 95 °C for 5 min, and separated on a 15% SDS–PAGE gel. The separated proteins were transferred to a polyvinylidene difluoride membrane (BioRad), and incubated with the specific primary antibodies, rabbit anti-SOD1 antibody (StressGen Biotechnologies, Victoria, British Columbia, Canada) and mouse anti-GAPDH

monoclonal antibody (Biodesign, Saco, ME, USA). After incubation, the membrane was rinsed and incubated with 0.1% horseradish peroxidase conjugated secondary antibodies, goat anti-rabbit HRP IgG and goat anti-mouse HRP IgG (Thermo Science, Rockford, IL, USA). Protein–antibody interactions were visualized using the supersignal west femto maximum sensitivity substrate (Thermo Science).

2.8. Pathological examinations

The skeletal muscles were frozen rapidly in liquid-nitrogen-cooled isopentane, and the liver and cardiac muscles were fixed in 10% formalin and embedded in paraffin. Ten-microgram frozen sections of skeletal muscles and 5-μm paraffin sections of liver and cardiac muscle were processed for hematoxylin and eosin staining.

2.9. Blood chemistry examinations

The sera were prepared from blood samples of the mice. In order to evaluate liver and muscle function, serum alanine aminotransferase (ALT), aspartate aminotransferase (AST), alkaline phosphatase (ALP), lactate dehydrogenase (LDH), total bilirubin (T-BIL), albumin (ALB), total protein (TP), and creatine kinase (CK) were measured (Oriental Yeast Co. Ltd., Tokyo, Japan). Statistically significant differences between the injected group and the control group were calculated by the Welch's *T*-test.

3. Results

3.1. Growth and health status of the injected mice

After the mice were injected with anti-SOD1 shRNA AAV9, they were raised together with their littermate controls for 4 weeks. The body weights of the injected mice and their littermate controls were similar (Fig. 2A). In the accelerating rotarod tests, there were no significant differences in motor function between the injected mice and littermate controls (Fig. 2B). At the end of the experimental period, the mice were dissected and showed no morphological abnormalities such as hepatomegaly, cardiomegaly, ascites, pleural effusion, edema, body fluid retention, or adhesion of organs.

3.2. Tissue expression of anti-SOD1 shRNA

Expression of anti-SOD1 shRNA in the liver, quadriceps, hamstrings and cardiac muscles was demonstrated by northern blot analysis (Fig. 3A). Fifty-four nucleotides (nt) of shRNA were not detected in these tissues (data not shown); however, a 21-nt antisense strand of siRNA was detected. This finding clearly indicates that the expressed anti-SOD1 shRNA was almost completely processed by Dicer. The expression level of the antisense siRNA was robust in cardiac and hamstring muscles, but surprisingly, much less in quadriceps muscles. Importantly, expression of siRNA was not detected in the liver.

3.3. The inhibitory effect of SOD1 mRNA

Quantitative RT-PCR showed that the expression level of SOD1 mRNA in the cardiac and hamstrings muscles of the injected mice was significantly reduced in comparison with those of the littermate controls. Using this method of injection, we observed approximately 80% reduction of SOD1 mRNA in the cardiac muscles and 65% reduction in the hamstrings. However, reduction of SOD1 mRNA in the quadricep muscles and liver were mild or absent (Fig. 3B). Effective suppression of the SOD1 gene was also confirmed at the protein level by Western blot analysis. Expression of the SOD1 protein was markedly reduced in the cardiac and hamstring muscles, but reduction in the liver was not clear (Fig. 3C).

3.4. Pathological examinations

HE staining of the injected mouse specimens showed no inflammatory changes in cardiac and skeletal muscles or in the liver (Fig. 4). In the hamstring muscle, we found no abnormal fibers such as small angular fibers, necrotic or regenerative muscle fibers. In the cardiac muscle, abnormal findings such as interstitial proliferation and muscle fiber degeneration were not seen. In the liver pathology, we found no structural abnormalities such as hepatic lobules.

3.5. Blood chemistry examinations

Serum AST, ALT, ALP, LDH, CK, ALB and TP values in both groups are shown in Table 1. Serum AST, ALT and LDH were increased

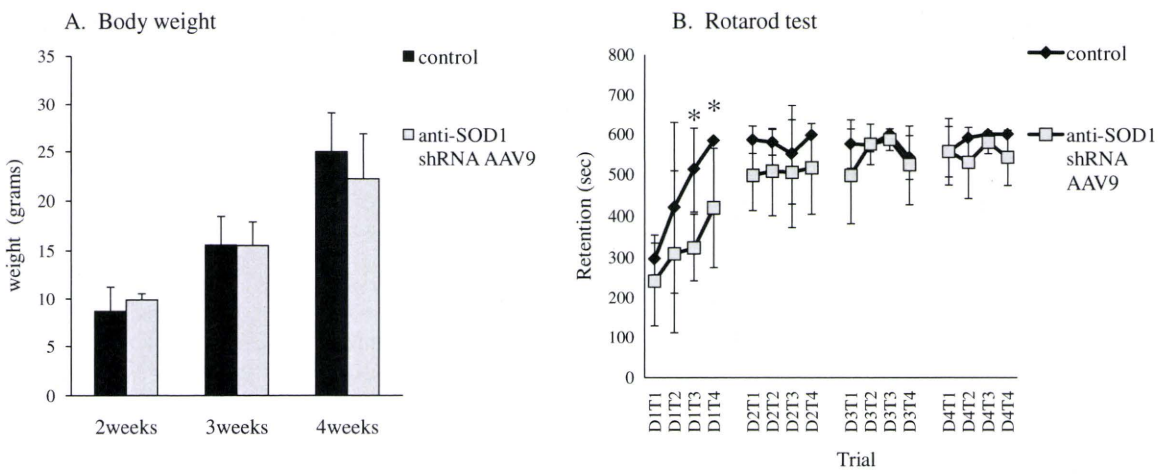

Fig. 2. Mouse growth and movement ability. (A) During the 4-week experimental period, none of the anti-SOD1 shRNA AAV9 vector-injected mice showed any significant differences in body weight compared with the littermate controls. Data are presented as the mean with SD ($n = 4$ for each group, $p > 0.05$). (B) In the accelerating rotarod test 4 weeks after injection of the anti-SOD1 shRNA AAV9 vector, all of the mice could perform the task similar to that of the littermate controls. Each mouse was trained in four trials each day (T1–T4), for a series of 4 days (D1–D4). Except for the third and fourth test of the first day (in the D1T3 $p = 0.025$, in the D1T4 $p = 0.048$), there was no significant difference between the injected mouse group and the littermate control group. Data are presented as the mean with SD ($n = 4$ for each group, $p > 0.05$).

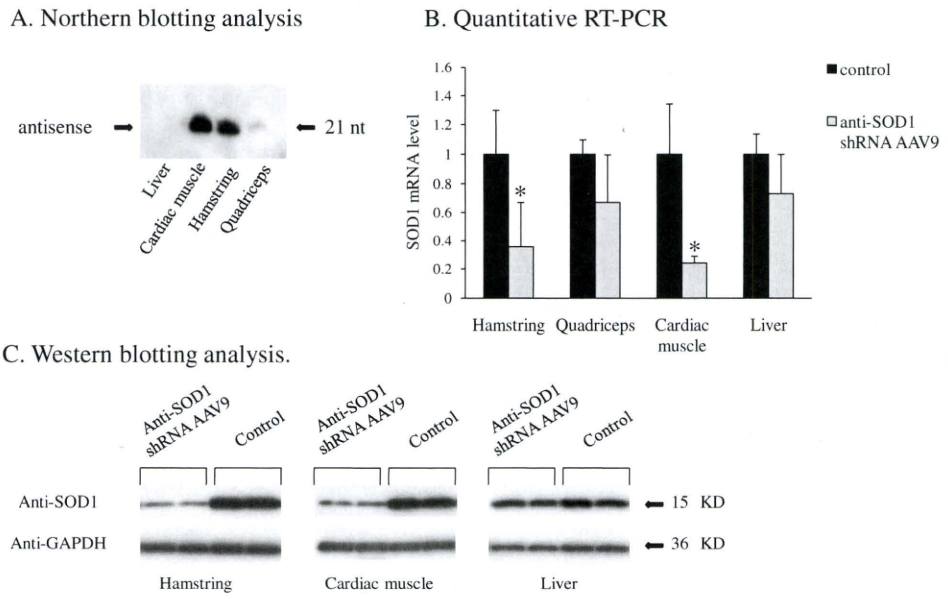

Fig. 3. Expression of shRNA and reduction efficiency of the anti-SOD1 shRNA AAV9 vector. (A) Northern blotting analysis of the total RNA derived from the liver, quadriceps, hamstrings, and cardiac muscles at 4 weeks after injection. The 21 nt antisense bands processed from shRNA are detected. Anti-SOD1shRNA is expressed higher in cardiac and hamstring muscles but shows lower expression in quadricep muscle and liver. (B) Quantitative RT-PCR of SOD1 mRNA in the liver, hamstrings, quadriceps, and cardiac muscles at 4 weeks after injection. SOD1 mRNA expression is significantly inhibited in cardiac and hamstring muscles. Data are presented as the mean with SD ($n = 4$ for each group, $p < 0.05$ only in the hamstring and heart). (C) The SOD1 protein was also reduced in cardiac and hamstring muscles but not in the liver, as assessed by Western blotting analysis at 4 weeks after injection.

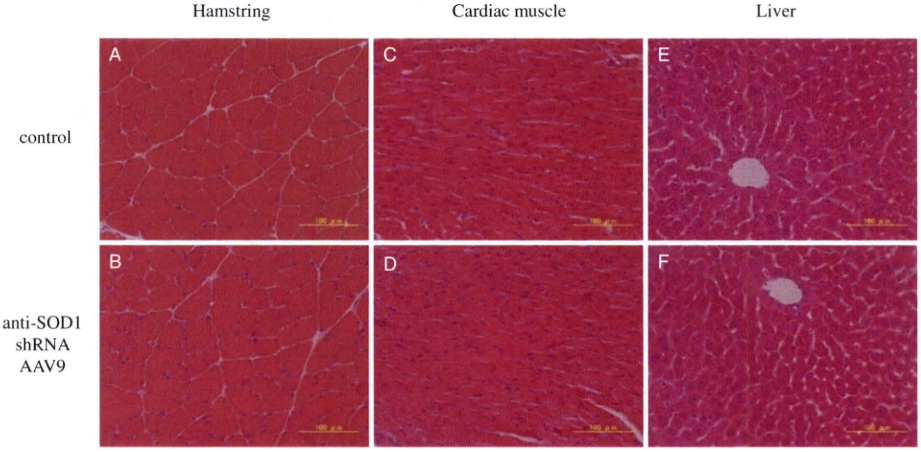

Fig. 4. Pathological examination. Photomicrographs of hematoxylin and eosin staining show no abnormalities in the hamstring (A and B), the cardiac muscle (C and D), and the liver (E and F). There were no alterations of cell size or shape, or infiltration of inflammatory cells in both of the groups (scale bar: 100 μm).

Table 1
Blood chemistry examinations.

Group	AST (IU/L)	ALT (IU/L)	ALP (IU/L)	LDH (IU/L)	CK (IU/L)	ALB (g/dL)	TP (g/dL)
Control	36 ± 7	16.8 ± 2.2	275.8 ± 65.3	574.5 ± 60.3	143.8 ± 29.9	1.7 ± 0.1	2.5 ± 0.2
Anti-SOD1 shRNA AAV9	56 ± 22.1	25.3 ± 11.2	273.8 ± 62.8	649.3 ± 237.1	215.8 ± 121.9	1.8 ± 0.1	2.6 ± 0.1

Mouse body weights were measured 4 weeks after anti-SOD1 shRNA AAV9 vector intraperitoneal injection. Alanine aminotransferase (ALT), aspartate aminotransferase (AST), alkaline phosphatase (ALP), lactate dehydrogenase (LDH), albumin (ALB), serum total protein (TP), creatine kinase (CK). The values are shown as mean ± SD ($n = 4$ in each group, the data of these examinations showed no significant differences between the anti-SOD1 shRNA AAV9 injected mouse group and the littermate control group, $p > 0.05$).

slightly in the anti-SOD1 shRNA AAV9-injected mouse group compared to that in the control littermate group. However, the values in the injected group were within the normal range, and this slight increase was not significant when compared with the littermate control group. Furthermore, serum CK level was also not significantly increased in the injected mice group. These data show that the injected mice could grow and develop without any side effects of the anti-SOD1 shRNA AAV9 vector.

4. Discussion

We report that systemic injection of shRNA AAV can inhibit target gene expression in skeletal and cardiac muscle without any adverse side effects. Previous reports state that AAV1, 6, 7, 8 and 9 can deliver specified genes efficiently to skeletal and cardiac muscle [7–10]. However, there is only one report showing significant inhibition in muscles by systemic injection of the shRNA AAV type

6 vector [12]. One explanation for the difficulty with reducing target gene expression in skeletal muscles is liver toxicity of high-dose shRNA as it potentially interferes with the miRNA system [1,4]. Thus, a sufficient dose of shRNA-AAV to effectively reduce target gene expression in skeletal muscles has not been administered, and in previous reports there has been no detailed description about liver dysfunction. The expression of shRNA is reportedly much higher in the liver than in any other tissues; however, shRNA efficacy in the liver is lower than in skeletal muscles [12], which implies the possibility of liver dysfunction. In this study, we effectively reduced our target gene in skeletal muscles by using neonatal mice. In contrast to the previous reports, in our study, northern blot analysis demonstrated almost no expression of shRNA in the liver, which explained the normal liver function that we saw in our mice. Though the mechanism for escaping liver toxicity is not well documented, a few reports have discussed that in neonates the high transduction efficiency in the liver is followed by rapid degradation during liver growth and cell division [9,15]. Our results of high reduction in hamstring muscle but low reduction in liver also indicate that the difference of the dividing or non-dividing characteristic of tissues could influence the efficacy of shRNA AAV in neonates.

Moreover, to evaluate liver function, we included two additional examinations. The first examination was a blood chemical evaluation measuring serum AST, ALT, etc. We found slightly increased serum AST, ALT and LDH in the injected mice; however, these values were within the normal range and were not statistically significant in comparison with the values of the littermate control group. The second examination was liver pathology. We found no morphological liver abnormalities such as swelling or atrophy, and could not find any inflammatory changes or destruction of hepatic lobules, microscopically. From these evaluations, we concluded that intraperitoneal injection of shRNA AAV into neonates does not induce any liver dysfunction.

We noted a difference in the expressed level of siRNA and the reduction rate of SOD1 gene between hamstring muscles and quadricep muscles. A few reports have discussed the difference in efficacy of AAV-delivered gene transduction among the skeletal muscles [6,9,10,15,19], but the reasons behind this remained uncertain. We believe that some of the reasons are as follows: different fiber type; the expression rate for AAV receptors may be different in each muscle; the pathway of systemic AAV circulation might affect the delivery; and the characteristics of U6 promoters might influence the AAV-delivered gene transduction in skeletal muscles.

Some studies discuss the relationship between AAV transduction and muscle fiber typing [6,15,19]; however, our results did not show such a correlation (data not shown). Considering AAV circulation, one report describes the correlation between the silencing effects and capillary density in the skeletal muscles, whereby the authors concluded that AAV circulation might not affect the difference seen among skeletal muscles [10]. AAV receptors have not yet been clearly identified. One of the receptors, the laminin receptor, has been analyzed in skeletal muscle, but the difference in the muscles was unaffected by this receptor alone [10]. Further studies are necessary to clarify the mechanisms behind the difference of gene targeting in muscle tissues, with one way to resolve this problem being the generation of systemic skeletal muscle disease animal models using the method described in this study.

We consider that the method used in this study offers a novel way to generate conditional knockdown in vivo models in certain skeletal and cardiac muscle tissue diseases. In particular, in some causative gene knockout models, it is very difficult to establish embryonic lethality, such as with the UDP-*N*-acetylglucosamine 2-epimerase/*N*-acetylmannosamine kinase (GNE) gene in distal myopathy with rimmed vacuoles (DMRV)/hereditary inclusion body myopathy (hIBM) [20,21], and Angiopoietin-1 gene related to prominent defects in endocardial and myocardial development [22]. To circumvent this limitation, reducing the target protein after birth might be a very powerful method for generating conditional knockdown models. In this study, we effectively reduced SOD1 gene expression in skeletal muscles, without any muscle damage. During the entire growth course of the mice, we did not observe growth retardation, abnormal motor ability, signs of heart or hepatic failures, or abnormal biochemical and pathological findings that would indicate the degeneration of skeletal and cardiac muscles in these injected mice. These results suggest that this shRNA AAV intraperitoneal injection method may not involve the liver, thus allowing us to examine the knockdown effects of our target gene in skeletal and cardiac muscles specifically.

Although we confirmed the gene-silencing effect in the muscles up to 2 months (data not shown), we did not examine how long the silencing effect would potentially last. It has been reported that shRNA transgenic mice with the same shRNA used in this study showed marked suppression of SOD1 for more than 1 year [3]. However, protein expressed by systemically injected AAV has been reported to reduce in humans within months, probably due to immunological elimination by CD8 memory T cells [23]. Although we considered there to be no memory CD8 T cells in our system because we injected the AAV just 1 day after birth, we still need to confirm the duration of the silencing effect.

Finally, we need to confirm the long-term safety of AAV and shRNA. Since the transduction or reduction of the target genes systemically is a very attractive method of gene therapy in skeletal muscle disease, this delivery system is useful not only for generating knockdown mouse models, but also for gene therapy of congenital cardiac and skeletal muscle disease.

Acknowledgments

This study was supported by the Research Grant (20B-13) for Nervous and Mental Disorders from the Ministry of Health, Labour and Welfare.

References

[1] J.J. Rossi, Expression strategies for short hairpin RNA interference triggers, Hum. Gene Ther. 19 (2008) 313–317.
[2] X. Gao, P. Zhang, Transgenic RNA interference in mice, Physiology 22 (2007) 161–166.
[3] Y. Saito, T. Yokota, T. Mitani, K. Ito, M. Anzai, M. Miyagishi, K. Taira, H. Mizusawa, Transgenic small interfering RNA halts amyotrophic lateral sclerosis in a mouse model, J. Biol. Chem. 52 (2005) 42826–42830.
[4] D. Grimm, K.L. Streetz, C.L. Jopling, T.A. Storm, K. Pandey, C.R. Davis, P. Marion, F. Salazar, M.A. Kay, Fatality in mice due to oversaturation of cellular microRNA/short hairpin RNA pathways, Nature 25 (2006) 537–541.
[5] T.R. Magee, J.N. Artaza, M.G. Ferrni, D. Vermet, F.I. Zuniga, L. Cantini, S. Reisz-Porszasz, J. Rajfer, N.F. Gonzalez-Cadavidm, Myostatin short interfering hairpin RNA gene transfer increases skeletal muscle mass, J. Gene Med. 8 (2006) 1171–1181.
[6] J.P. Louboutin, L. Wang, J.M. Wilson, Gene transfer into skeletal muscle using novel AAV serotypes, J. Gene Med. 7 (2005) 442–451.
[7] C. Zincarelli, S. Soltys, G. Rengo, J.E. Rabinowitz, Analysis of AAV serotypes 1–9 mediated gene expression and tropism in mice after systemic injection, Mol. Ther. 16 (2008) 1073–1080.
[8] M.J. Blankinship, P. Gregorevic, J.M. Allen, S.Q. Harper, H. Harper, C.L. Halbert, A.D. Miller, J.S. Chamberlain, Efficient transduction of skeletal muscle using vectors based on adeno-associated virus serotype 6, Mol. Ther. 10 (2004) 671–678.
[9] Z. Wang, T. Zhu, C. Qiao, L. Zhou, B. Wang, J. Zhang, C. Chen, J. Li, X. Xiao, Adeno-associated virus serotype 8 efficiently delivers genes to muscle and heart, Nat. Biotechnol. 23 (2005) 321–328.
[10] Y. Yue, A. Ghosh, C. Long, B. Bostick, B.F. Smith, J.N. Komegay, D.A. Duan, A single intravenous injection of adeno-associated virus serotype-9 leads to whole body skeletal muscle transduction in dogs, Mol. Ther. 16 (2008) 1944–1952.
[11] K. Inagaki, S. Fuess, T.A. Strom, G.A. Gibson, C.F. Mctiernan, M.A. Kay, H. Nakai, Robust systemic transduction with AAV9 vectors in mice: efficient global cardiac gene transfer superior to that of AAV8, Mol. Ther. 14 (2006) 45–53.

[12] C. Towne, C. Raoul, B.L. Schneider, P. Aebischer, Systemic AAV6 delivery mediating RNA interference against SOD1: neuromuscular transduction does not alter disease progression in fALS mice, Mol. Ther. 16 (2008) 1018–1025.
[13] T. Ogura, H. Mizukami, J. Mimuro, S. Madoiwa, T. Okada, T. Matsushita, M. Urabe, A. Kume, H. Hamada, H. Yoshikawa, Y. Sakata, K. Ozawa, Utility of intraperitoneal administration as a route of AAV serotype 5 vector-mediated neonatal gene transfer, J. Gene Med. 8 (2006) 990–997.
[14] K.D. Foust, A. Poirier, C.A. Pacak, R.J. Mandel, T.R. Flotte, Neonatal intraperitoneal or intravenous injection of recombinant adeno-associated virus type 8 transduce dorsal root ganglia and lower motor neurons, Hum. Gene Ther. 19 (2008) 61–70.
[15] B. Bostick, A. Ghosh, Y. Yue, C. Long, D. Duan, Systemic AAV-9 transduction in mice is influenced by animal age but not by the route of administration, Gene Ther. 14 (2007) 1605–1609.
[16] K.D. Foust, E. Nurre, C.L. Montgomery, A. Hernandez, C.M. Chen, B.K. Kaspar, Intravascular AAV9 preferentially targets neonatal neurons and adult astrocytes, Nat. Biotechnol. 27 (2009) 59–65.
[17] T. Yokota, M. Miyagishi, T. Hino, R. Matsumura, A. Tasinato, M. Urushitani, R.V. Rao, R. Takahashi, D.E. Bredesen, K. Taira, H. Mizusawa, SiRNA-based inhibition specific for mutant SOD1 with single nucleotide alternation in familial ALS, compared with ribozyme and DNA enzyme, Biochem. Biophys. Res. Commun. 314 (2004) 283–291.
[18] W.T. Hermens, O. Ter Brake, P.A. Dijkhuizen, M.A. Sonnemans, D. Grimm, J.A. Kleinschmidt, J. Verhaagen, Purification of recombinant adeno-associated virus by iodixanol gradient ultracentrifugation allows rapid and reproducible preparation of vector stocks for gene transfer in nervous system, Hum. Gene Ther. 10 (1999) 1885–1891.
[19] C.A. Pacak, T. Conlon, C.S. Mah, B.J. Byme, Relative persistence of AAV serotype 1 vector genomes in dystrophic muscle, Genet. Vaccines Ther. 6 (2008) 14.
[20] M. Schwarzkopf, K.P. Knobeloch, E. Rohde, S. Hinderlich, N. Wiechens, L. Lucka, I. Horak, W. Reutter, R. Horstkorte, Sialylation is essential for early development in mice, Proc. Natl. Acad. Sci. USA 99 (2002) 5267–5270.
[21] M.C. Malicdan, S. Noguchi, I. Nonaka, Y. Hayashi, I. Nishino, A Gne knockout mouse expressing human GNE D176V mutation develops features similar to distal myopathy with rimmed vacuoles or hereditary inclusion body myopathy, Hum. Mol. Genet. 16 (2007) 2669–2682.
[22] C. Suri, P.F. Jones, S. Patan, S. Bartunkova, P.C. Maisonpierre, S. Davis, T.N. Sato, G.D. Yancopoulos, Requisite role of angiopoietin-1, a ligand for the TIE2 receptor, during embryonic angiogenesis, Cell 87 (1996) 1171–1180.
[23] C.S. Manno, G.F. Pierce, V.R. Arruda, B. Glader, M. Ragni, J.J. Rasko, M.C. Ozelo, K. Hoots, P. Blatt, B. Konkle, M. Dake, R. Kaye, M. Razavi, A. Zajko, J. Zehnder, P.K. Rustagi, H. Nakai, A. Chew, D. Leonard, J.F. Wright, R.R. Lessard, J.M. Sommer, M. Tigges, D. Sabatino, A. Luk, H. Jiang, F. Mingozzi, L. Couto, H.C. Ertl, K.A. High, M.A. Kay, Successful transduction of liver in hemophilia by AAV-Factor IX and limitations imposed by the host immune response, Nat. Med. 12 (2006) 342–347.

HUMAN GENE THERAPY 00:1–9 (XXXXX 2011)

DOI: 10.1089/hum.2010.083

High-Density Lipoprotein Facilitates *In Vivo* Delivery of α-Tocopherol–Conjugated Short-Interfering RNA to the Brain

Yoshitaka Uno,[1] Wenying Piao,[1] Kanjiro Miyata,[2] Kazutaka Nishina,[1] Hidehiro Mizusawa,[1] and Takanori Yokota[1]

Abstract

We originally reported the use of vitamin E (α-tocopherol) as an *in vivo* vector of short-interfering RNA (siRNA) to the liver. Here, we apply our strategy to the brain. By combining high-density lipoprotein (HDL) as a second carrier with α-tocopherol–conjugated siRNA (Toc-siRNA) in the brain, we achieved dramatic improvement of siRNA delivery to neurons. After direct intracerebroventricular (ICV) infusion of Toc-siRNA/HDL for 7 days, extensive and specific knock-down of a target gene, β-site amyloid precursor protein cleaving enzyme 1 (*BACE1*), was observed in both mRNA and protein levels, especially in the cerebral cortex and hippocampus. This new delivery method achieved a much more prominent down-regulation effect than conventional silencing methods of the brain gene, i.e., ICV infusion of nonconjugated siRNA or oligonucleotides. With only 3 nmol Toc-siRNA with HDL, BACE1 mRNA in the parietal cortex could be reduced by ~70%. We suppose that this dramatic improvement of siRNA delivery to the brain is due to the use of lipoprotein receptor–mediated endocytosis because the silencing efficiency was significantly increased by binding of Toc-siRNA to the lipoprotein, and in contrast, was clearly decreased in lipoprotein-receptor knockout mice. These results suggest exogenous siRNA could be used clinically for otherwise incurable neurological diseases.

Introduction

THE POSSIBLE THERAPEUTIC APPLICATIONS of short-interfering RNA (siRNA) cover a wide spectrum of disorders, including cancer, infectious diseases, and inherited diseases. There has been much interest in the clinical applications of siRNA to neurological diseases such as Alzheimer's disease (AD), Huntington's disease, Parkinson's disease, and amyotrophic lateral sclerosis. However, delivery of siRNA to the brain has not been well established.

For *in vivo* delivery of siRNA, viral vectors and high-pressure, high-volume intravenous injection methods have been described. However, these approaches have limitations in clinical practice due to their side effects. Much progress has been reported on intravenous administration of siRNA to the liver using cationic liposomes, nanoparticles, and cell-penetrating peptides (Zimmermann *et al.*, 2006; Moschos *et al.*, 2007; Rozema *et al.*, 2007; Wolfrum *et al.*, 2007; Akinc *et al.*, 2008, 2009; Gao *et al.*, 2009). Ligand conjugation for receptor-mediated uptake system is also expected to be another possible delivery method *in vivo* (Kumar *et al.*, 2007).

We recently published a report of efficient systemic delivery of siRNA to the liver by using conjugation with α-tocopherol (Nishina *et al.*, 2008). We expected that the most effective *in vivo* carrier would be a molecule that is essential for target tissue cells but cannot be synthesized within the cells. Vitamins fit these requirements well, and the least toxic vitamin, even at high doses, is vitamin E (Kappus and Diplock, 1992). α-Tocopherol is a lipophilic natural molecule and has physiological pathways from blood to the brain as well as to the liver. Orally ingested α-tocopherol is absorbed at the ileum, incorporated into chylomicrons, and transferred to very-low-density lipoprotein (VLDL) in the liver by α-tocopherol transfer protein (αTTP). VLDL containing α-tocopherol is metabolized to low-density lipoprotein (LDL) and HDL, which supply α-tocopherol to all tissue cells via their respective lipoprotein receptors (Rigotti, 2007). The delivery pathway of α-tocopherol to the brain has not been

[1]Department of Neurology and Neurological Science, Graduate School, Tokyo Medical and Dental University, Bunkyo-ku, Tokyo 113-0034, Japan.
[2]Division of Clinical Biotechnology, Center for Disease Biology and Integrative Medicine, Graduate School of Medicine, The University of Tokyo, Bunkyo-ku, Tokyo 113-0034, Japan.